

---

# 20 Scaling and Hierarchy of Models for Flow Processes in Unsaturated Fractured Rock

*B. Faybishenko, G.S. Bodvarsson, J. Hinds,  
and P.A. Witherspoon*

## CONTENTS

I. Introduction.....	374
A. Problem Statement and Definitions.....	374
B. Goals and Structure .....	374
II. Causes of Complexity in Investigations of Flow and Transport through Unsaturated Fractured Rock .....	375
A. Definition of Complexity.....	375
B. Complexity of Flow and Transport Processes .....	375
C. Limitations of Monitoring Methods for Unsaturated Fractured Rock .....	377
1. Types of Measurements .....	377
2. Limitations of Field Measurements .....	378
3. Core Investigations .....	379
III. Background of Scaling and Hierarchy Theory .....	379
A. Theory of Scaling for Saturated and Unsaturated Media.....	379
1. Saturated Media.....	380
2. Unsaturated Soils.....	381
3. Unsaturated Fractured Media .....	382
B. Effective Hydraulic Parameters for Heterogeneous Media .....	384
C. Hierarchy Approach.....	385
IV. Examples of Investigations of Fractured Rock.....	388
A. Fractured Basalt of the Snake River Plain, Idaho .....	388
1. Geologic Conditions .....	388
2. Hierarchical Scales for Fractured Basalt.....	388
3. Infiltration Tests on a Hierarchy of Scales.....	391
B. Fractured Tuff at Yucca Mountain.....	395
1. Geologic Conditions and Types of Fracture Patterns .....	395
2. Relationship between Hierarchical Components for Fractured Tuff.....	397
3. Infiltration and Air-Injection Tests on a Hierarchy of Scales.....	401
V. Models of Flow Processes on a Hierarchy of Scales .....	404
A. Types of Models .....	404
B. Examples of Models.....	405
1. Elemental Scale .....	405
2. Small Scale .....	405
3. Intermediate Scale .....	406

4. Large Scale .....	407
VI. Discussion and Conclusions .....	407
VII. Acknowledgments .....	409
References .....	409

## I. INTRODUCTION

### A. PROBLEM STATEMENT AND DEFINITIONS

The fact that similar objects appear different depending on the scale of observation is well known and has important scientific and practical implications for earth sciences. Pore-scale information describing subsurface processes is more than likely to be irrelevant for predicting such processes at the kilometer scale. The need for a multiscale representation of subsurface processes arises when dealing with large and complex subsurface volumes, such as when performing field-scale experimental and modeling investigations of flow processes in unsaturated fractured rock.

*Scale* can be defined as part of a system (e.g., characteristic length, area, volume, time) from which the system is observed. The problem of relating physical processes that occur on different spatial and temporal scales is called *bridging the scales*.<sup>1</sup> One of the approaches to bridging the scales is *scaling*. Scaling can be defined as a relationship representing how system's features change with the size (scale) of the system. The interpretation of information across scales, including scaling-up (from fine to coarse scale) and scaling-down (from coarse to fine), is important for many ecological systems,<sup>2</sup> soils,<sup>3-6</sup> and fractured-rock sites.<sup>7-9</sup> A great deal of field, laboratory, and modeling research related to flow and transport in heterogeneous soils and fractured rock has been performed on a variety of scales ranging from a single fracture to large (kilometer-scale) parts of geological media. (This research is to a large degree summarized in monographs.<sup>5,10-16</sup>) Still, scaling problems are far from being resolved. One of the reasons for this lack of resolution is that most laboratory and field investigations have been carried out over relatively small areas (<1 m<sup>2</sup>) and during short time periods. Consequently, these results have been extrapolated to larger spatial (>10<sup>3</sup> m<sup>2</sup>) and time scales using insufficiently validated theoretical models.<sup>6</sup>

Scaling laws that are useful for simple homogeneous or heterogeneous porous systems may fail for fractured rock.<sup>17</sup> This happens for two main reasons. First, a variety of processes control flow in fractured rock (often containing geological discontinuities such as faults and fractures) at different scales<sup>18</sup> and, second, we are unable to directly monitor various parameters describing nonlinear interactions, time delays, or feedback between rock discontinuities and the matrix. One of the alternative approaches that can be used to handle the problem of scale (and scaling) is based on the concept of *hierarchy of scales*.

*Hierarchy* represents a system structure or the classification of a graded (ranked) series of system parts (subsystems), with each subsystem dominant over those below it and controlled by those above it. Hierarchy theory is one of the main theoretical approaches used in systems analysis, dealing with complex, multiscaled systems.<sup>19,20</sup> This theory has been extensively applied to various ecological and biological systems.<sup>2,21-28</sup> Wagenet and Hutson<sup>29</sup> used an 11-level hierarchy of scales for soil-science investigations. Such an approach was also used to describe hydrologic processes.<sup>30</sup> A hierarchical approach was applied to describe flow processes in unsaturated soils under irrigation.<sup>31</sup> Faybishenko et al.<sup>32</sup> have also attempted to characterize a hierarchy of scales for flow and transport in fractured basalt. However, despite a number of publications on the hierarchical approach, practical applications of this concept in soil sciences and hydrogeology are still limited.

### B. GOALS AND STRUCTURE

Soil scientists and hydrogeologists are faced with the question of whether flow processes in unsaturated fractured rock can be analyzed using the same measurements and models, regardless of the scale of the problem. To answer this question, the goals of this chapter are to review existing

scaling approaches and to describe a concept for a hierarchy of scales that can be used for spatial–temporal investigations of unsaturated flow and transport in fractured rocks, including elemental-, small-, intermediate-, and large-scale investigations. We will demonstrate the effectiveness of a triadic hierarchical structure in describing flow and transport in unsaturated fractured rock, in which each level of the hierarchy includes investigations at least one level above the level of interest (to determine boundary conditions) and one level below the level of interest (to determine parameters of equations). The application of this methodology requires different conceptual approaches to site characterization and modeling at different scales. We will illustrate the theoretical concepts using results from field investigations of fractured basalt in the Snake River Plain, Idaho, and fractured tuff at Yucca Mountain, Nevada.

Section II presents a general description of complex flow processes in fractured rock, including the geometry and physics of flow and the limits of existing monitoring methods. Section III reviews scaling and hierarchical approaches in analyzing complex systems and emphasizes the difference between these approaches. Section IV presents the results of investigations (based on air-injection and infiltration tests) in fractured basalts (near INEEL, Idaho) and fractured tuffs (potential nuclear waste disposal site at Yucca Mountain, Nevada), while Section V summarizes the models on a hierarchy of scales. Section VI presents a discussion and conclusions.

## II. CAUSES OF COMPLEXITY IN INVESTIGATIONS OF FLOW AND TRANSPORT THROUGH UNSATURATED FRACTURED ROCK

### A. DEFINITION OF COMPLEXITY

Complexity in investigations of flow and transport in fractured rock results from the combined effect of flow processes and observational uncertainties. According to *Webster's Dictionary*, the term *complex* means “a whole made up of complicated or interrelated parts.” Key elements causing complex flow processes are the geometry and physics of flow in fractures, discussed in Section II.B. An insufficient resolution of measurements (a typical difficulty in field characterization methods) leads to an inability to detect multiple, complex processes occurring in single fractures or a fracture network, as will be discussed in Section II.C. Modeling the different physical processes involved in flow and transport through fractured rock, using a considerable number of physical variables, belongs to a class of problems called *organized complexity*.<sup>33</sup>

### B. COMPLEXITY OF FLOW AND TRANSPORT PROCESSES

Complexity of flow and transport processes in unsaturated rock and soils is caused by a variety of processes, such as preferential and fast flow in fractures, funneling and divergence of localized and nonuniform flow paths, nonlinearity of hydraulic processes, unstable and chaotic flow, liquid film flow along a fracture surface, intrafracture water dripping, fractional-dimensional flow, and fracture–matrix interaction. For example, preferential/fast flow of water has been reported along localized pathways in soils<sup>31,34–36</sup> and in fractured rocks.<sup>37–40</sup> Preferential water flow is caused for a variety of reasons, such as heterogeneities at different scale,<sup>41,42</sup> wetting-front instabilities and fingering,<sup>43–47</sup> flow through macropores, water repellence in dry soils, nonuniform areal distribution of infiltration at the land surface, air entrapment in soils<sup>48,49</sup> and fractured rock.<sup>50</sup> Often many, or in some cases nearly all, observable fractures play no significant role in water flow, even when they appear to be interconnected. Field and laboratory studies revealed that fractures may become nonconductive because apertures are closed, either partially or completely, under the ambient stress state or by mineral precipitation, biofilm clogging, sealing, or air entrapment<sup>48,49</sup>

Funneling and divergence of highly localized and extremely nonuniform water flow paths were detected in laboratory experiments in fracture models<sup>46,47,51,52</sup> and in field experiments affected by the geometry of the fracture network.<sup>37,50</sup> [Figure 20.1](#)<sup>53</sup> illustrates a variety of local flow patterns at different

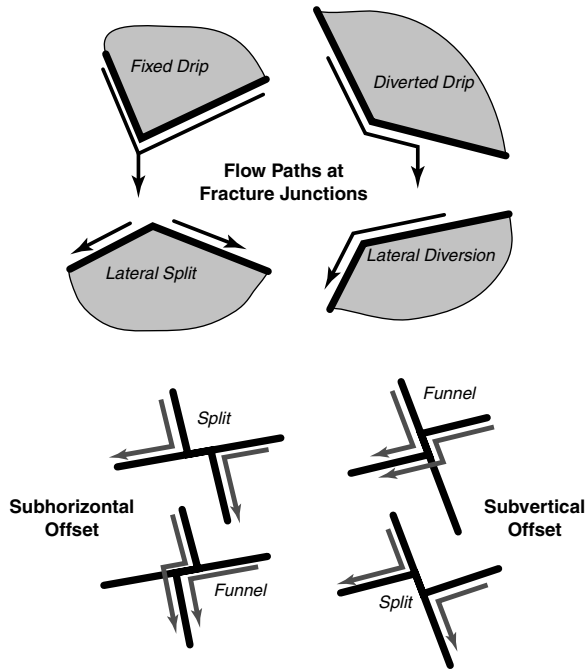


**FIGURE 20.1** Examples of patterns of film flow and dripping behavior at fracture junctions (Stothoff, S. and Or, D.A., in *Dynamics of Fluids in Fractured Rock*, B. Faybishenko, Witherspoon, P.A., and Benson, S.M., Eds., Geophysical Monograph 122, AGU, 267, 2000. American Geophysical Union. With permission.), demonstrating lateral diversion on hanging walls, which is flux dependent; routing into fractures, which is dependent on fracture capacity; anisotropy from diversion and funneling that may occur due to fracture offsets; and lateral diversion on hanging walls that may convert funnel configurations into split configurations. (American Geophysical Union. With permission.)

fracture junctions, with no similarity between the flow patterns. Funneling of water also causes the creation of local perched-water zones above low-permeability zones within heterogeneous media.<sup>50</sup> Water flow in a fracture network embedded in a low-permeability matrix depends strongly on the interconnections within the fracture system. Rock discontinuities are present on all scales, extending from the microfissures among the mineral components of the rock to the macroscale joints and faults.<sup>54</sup>

Nonlinearity of hydraulic processes is caused by nonlinear relationships among the moisture content, capillary pressure, and unsaturated hydraulic conductivity. These nonlinear functions are described, for example, by the well-known Brooks-Cory,<sup>55</sup> Gardner,<sup>56</sup> or van Genuchten<sup>57</sup> formulae, which render nonlinear forms of Darcy's law and Richards' equation (for unsaturated flow). Nonlinear relationships also characterize the dependence among tortuosity parameters and water and air contents in unsaturated media.<sup>58</sup> Nonlinearity is a necessary (but insufficient) condition for a system to be chaotic.<sup>59</sup>

The effects of capillary, viscous, and gravitational forces are relatively well understood for unsaturated porous media, but their coupled effects in fractured-porous media are not well understood and cause uncertainty in predictions of flow and transport. Unstable flow has been observed in laboratory experiments on water seepage through soil<sup>35,60</sup> and in fracture models,<sup>52,61,62</sup> as well as during field infiltration tests in fractured basalt<sup>63</sup> and fractured tuff.<sup>64</sup> An air and liquid pressure time series can be used to evaluate the presence of deterministic-chaotic and stochastic components in the data.<sup>65</sup> Unstable and chaotic flow processes in fractures are caused by a combination of pore-throat effects, fracture roughness, preferential flow, variable surface wetting, etc. However, these intrafracture flow processes do not have analogs on larger scales.

Furthermore, intrafracture roughness affecting flow, on the local scale, is neither geometrically nor physically analogous to the field-scale fracture pattern. Based on current experimental technologies, intrafracture measurements of water pressure, film thickness, or moisture content cannot be performed directly at the field scale.

Film flow in fractures is controlled by a combination of surface tension, gravity, and inertia and is bounded on one side of the fracture by the supporting solid matrix and on the other side by a fluid interface. If the surrounding fluid is gas, the film has a free surface. According to Tokunaga et al.,<sup>66</sup> film flow causes fast water flow in fractured rocks. Film-flow processes also depend on numerous factors, such as traces of impurities, roughness, temperature, contact angle of a drop,<sup>67</sup> and intrafracture water dripping.<sup>52</sup>

Fractional flow occurs in fractured rock because of discontinuities, which may change the dimensionality of flow with distance from a pumping/injection well.<sup>68–70</sup> In suggesting that a fracture network may cause fractal-dimensional flow, Barker<sup>68</sup> generalized Theis' classic solution for transient radial flow to a well including a noninteger, or fractal, flow dimension. Riemann et al.<sup>71</sup> and van Tonder et al.<sup>70</sup> used generalized equations with fractional-flow dimensions to estimate seepage velocities and to analyze single-well injection-withdrawal field tests. Pachepsky et al.<sup>72</sup> simulated scale-dependent solute transport in soils using the fractional advective-dispersive equation. Flow-channel geometry for water flow and hydraulic properties of porous and fractured media can be described by fractal models.<sup>73–76</sup> Fractal structures found in the geologic medium under investigation are also indicative of chaotic behavior.<sup>77,78</sup> For unsaturated media, the flow dimension can vary when new fractures or flow paths are involved in flow.

*Fracture-matrix interaction* is the term frequently used to identify water exchange between a fracture and the surrounding matrix. Flow in fractures can be retarded by matrix imbibition. The decreased area for water flow in unsaturated fractures was observed in laboratory experiments.<sup>46,47,52</sup> Three-dimensional modeling of the Box Canyon (Idaho) pneumatic and infiltration tests, using a dual-permeability approach, indicated that the fracture-matrix interfacial area combined with fracture-continuum porosity were very sensitive parameters that controlled water travel time.<sup>79</sup> The fracture-matrix continua interfacial area was scaled by a factor of 0.01, which indicates a decreased contact area of the water phase between the fracture and matrix resulting from the channelized flow through the variably saturated fractures. Despite the possibility of changing local geometry of flow over time,<sup>51,52</sup> the average coverage of these pathways along the fracture surface remains almost stable (over time) for constant boundary conditions. These results confirm the concept of a “self-organized” critical state,<sup>80</sup> in which the surface nonuniformly distributed water coverage has a critical value (despite the additional water supplied to the surface), and the system organizes in such a way that the excess water is removed by streams.

## C. LIMITATIONS OF MONITORING METHODS FOR UNSATURATED FRACTURED ROCK

### 1. Types of Measurements

The problem of scale is associated with measurement procedures.<sup>81</sup> To better understand flow processes in heterogeneous fractured rock from experiments, we must recognize the inherent features and limitations of different types of field and laboratory measurements. The point-type probes (e.g., tensiometers, thermistors, miniature electrical resistivity probes), which may or may not intersect single fractures and narrow zones of preferential flow, provide passive-type measurements by responding only to water contacting the probes. Tensiometers and suction lysimeters (using a vacuum to collect water for chemical analysis), with porous tips intersecting fractures and matrix, can create an artificial hydraulic connection between the fracture and matrix, changing the local flow paths in the vicinity of the probe. Tensiometer measurements can exhibit significant extrinsic hysteresis (caused by the water redistribution between the fracture and matrix, as well as by the delay time of the tensiometer), even without taking into account the intrinsic hysteresis of the unsaturated hydraulic fracture and matrix characteristics.<sup>82</sup> Because of complex three-dimen-

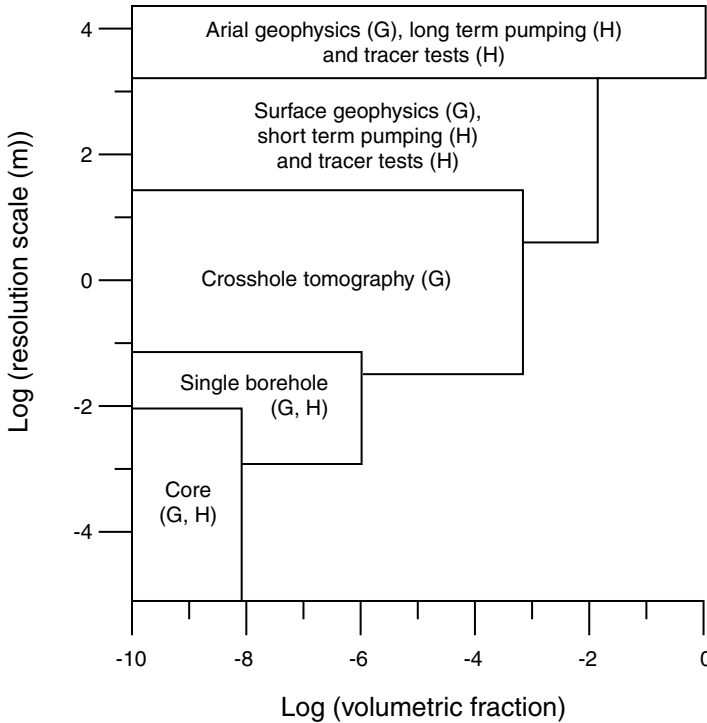


**FIGURE 20.2** Illustration of the relationship between the types of geophysical (G) and hydrogeological (H) measurements and the volume of rock involved in measurements with different techniques (From Hubbard, S. et al., in *Vadose Zone, Science and Technology Solutions*, Looney, B. and Falta, R., Eds., Batelle Press, 215, 2000.)

sional channelized preferential water flow, measurements of local water pressure using tensiometers are of limited use in evaluating hydraulic gradient and water flux in fractured rocks, if the probes are separated by a fracture. Volume-averaged, local tensiometer measurements can thus provide only a limited understanding of water travel time in fractured rocks and might lead to erroneous interpretations if used to directly assess the hydraulic gradient, direction of water flow, or moisture content of fractured rocks.

Moisture-content (saturation) measurements provide volume-averaged, near-borehole or cross-borehole measurements. For example, neutron logging provides measurements at locations 20 to 30 cm from a borehole. Geophysical methods, such as seismic survey, ground penetrating radar (GPR) and electrical resistivity tomography (ERT) can be used for cross-borehole imaging over distances of up to 10 to 12 m.<sup>83,84</sup> The resolution of geophysical methods depends on the volume of the subsurface involved, as demonstrated in Figure 20.2.

## 2. Limitations of Field Measurements

Despite providing spatially averaged data for subsurface conditions, the shortcoming of geophysical methods is their lack of fine resolution and the difficulty of directly correlating electromagnetic responses, seismic velocities, etc. with the physics of point-type measurements and hydrogeologic parameters governing fluid flow. The shortcoming of point-type probe and near-borehole measurements is the difficulty of combining their responses in a meaningful way, such as integrating or volume-averaging responses from a limited number of measurements. Because field measurements generally provide only average characteristics of rock and fracture properties over the surface of the monitoring sensor, the actual resolution of the measurements and the volume of rock involved

in averaging remain unknown. Neither field method can be used to observe flow in single fractures or the fracture-matrix interface in sufficient detail directly, nor can they distinguish between flow-through and dead-end fractures or determine the fracture-matrix interaction area (without inverse modeling). It is also important to emphasize the discrepancy between point-type measurements of water pressure, which are assumed to be at some “finger” scale, and the volume-averaged flux measurements, which are determined from the rate at which water flows through the cross section of media. For core investigations, the flux is measured on a “chamber” scale.<sup>46</sup> The same consideration is true for field ponded-infiltration tests, with water supplied into the subsurface through a certain surface area (see Section IV.A).

### 3. Core Investigations

Cores taken from the natural rock environment are likely to undergo changes in their structure, temperature, and porous space humidity. These changes may in turn affect unsaturated and saturated hydraulic parameters. Because of their limited size, cores do not usually include natural fractures or fracture junctions, but may characterize only local matrix properties or a limited area of the fracture-matrix interface. In his review of fracture properties from laboratory and large-scale field tests, Gale<sup>18</sup> concluded that a comparison of permeability data for crystalline rocks, from tests that range from laboratory size to regional scales, must take into account the difference in methods used to test the samples. The lower limit in the data reflects the scale effects; the upper limit reflects normal variations in permeability, as suggested by Neuman.<sup>85</sup> In this case, permeability increases as the size of the samples increases. Renshaw,<sup>86</sup> who compiled data for hydraulic conductivity of fractured rock from laboratory and field investigations, suggested that an increase in conductivity at the field scale, compared to conductivity from laboratory tests, could be caused by a systematic bias in laboratory-scale samples, which may not contain fractures any larger than the size of the sample. He also suggested that, because many fracture networks are near the percolation threshold, the conductivity of simulated networks in such cases is consistent with the compiled data and increases with the sample dimension.

Thus, the main limitations of experimental investigations of flow through unsaturated fractured rock arise from the inconsistency among the physics of measurements, using available instrumentation, and the physics of flow processes in fractured media. In other words, measurements are usually obtained at a smaller scale than that of processes that these measurements are attempting to characterize.

## III. BACKGROUND OF SCALING AND HIERARCHY THEORY

### A. THEORY OF SCALING FOR SATURATED AND UNSATURATED MEDIA

A simple scaling relationship representing changes in a system’s feature ( $y$ ) with scale ( $x$ ) is a power law given by<sup>163</sup>

$$y = cx^a \quad (20.1)$$

where  $c$  is a system-specific constant and  $a$  is the power that describes the relationship. If Equation 20.1 holds, the system is called self-similar. Scaling of a self-similar flow process is generally based on three conditions: (1) *physical* (dynamic and kinematic) *similarity* (for example, similarity criteria, expressing the relative importance of changing velocity, gravity, inertia, viscosity, and surface tension forces with scale); (2) *geometric similarity* (for example, expressing the similarity between the dimensions of areal and volumetric moisture distributions); and (3) *functional similarity* of models used for different scales.

## 1. Saturated Media

The hydraulic properties of saturated heterogeneous media are known to correlate with the scale of observations, from the size of a laboratory core to thousands of meters.<sup>85–90</sup> Scaling of hydraulic properties is, in general, based on a concept of fractal analysis.<sup>30,91</sup> Scaling for saturated permeability<sup>85</sup> and air permeability<sup>7</sup> becomes possible because of the geometrical similarity of continuous fractured porous media and a linear superposition of factors affecting saturated flow in different parts of the rock. Based on statistical analysis of experimental data, several studies have suggested that the relationship between hydraulic conductivity,  $K$ , and the volume of media is given by

$$K = cV^\alpha \quad (20.2)$$

where  $c$  is a parameter (which depends on formation properties such as pore size distribution or interconnectivity in porous media, and fracture aperture and fracture interconnectivity in fractured rock),  $V$  is the volume of the formation tested, and  $\alpha$  is a scaling exponent.

Neuman<sup>85,89</sup> and Di Federico and Neuman<sup>92</sup> determined that  $\alpha$  is 1/2. Assuming a fractal formation structure, Neuman<sup>85</sup> considered 131 points from tracer tests in field and laboratory conditions, including data from fractured rock sites, over a range of scales from 10 to 3500 m. Neuman was able to fit Equation 20.2 to these data with a regression coefficient  $R^2 = 0.74$  and a rather narrow 95% confidence interval. He was able to determine a single variogram,  $\gamma(s) = c\sqrt{s}$ , where  $s$  is the distance and  $c$  is the constant, for which all local semivariograms are expected to fluctuate with zero mean and a relatively large amplitude. The log hydraulic conductivities exhibit self-similarity in a global sense when large amounts of data from various hydrogeological settings are examined as a group. Assuming that a pore network preserves the total area and length from one level to another, Winter and Tartakovsky,<sup>93</sup> based on the work of West et al.,<sup>94</sup> derived Equation 20.2 with a scaling exponent of 1/2.

Neuman and Di Fredirico<sup>95</sup> presented an idea of an infinite hierarchy of a multiscale permeability field, based on a notion that permeability measurements are both random and uncertain, causing the partial differential equations to become stochastic. These authors indicated that randomness is caused by measurement's errors and its uncertainties. The latter is caused by measurements on different support scales characterizing different (selected) locations within discrete depth intervals. In this approach, the presence of a log–log relationship between the permeability and the support scale is considered indicative of a hierarchy of scales. Moreover, it is implied that the same equation governs flow processes in geologic media on different scales, and the only difference between measurement results is from the effect of different properties as the flow domain changes. (Note that the idea of the hierarchical approach to investigate water flow and transport in porous media by Neuman and Di Fredirico<sup>95</sup> and Wheatcraft and Cushman<sup>96</sup> is different from that we propose in Section III.C)

Schultze-Makuch et al.,<sup>97</sup> who studied the relationship between the hydraulic conductivity ( $K$ ) and the scale of measurement for various types of sediments and rocks, observed no variations in  $K$  with scale for homogeneous media (such as quartz sandstones). They reported that  $K$  increased with scale in heterogeneous media in confined and unconfined aquifers, and the scaling exponent for Equation 20.2 varied between 0.5 and 1.0, increasing in fractured rock. The value of  $K$  increased until the maximum as the scale reached a certain rock volume, after which  $K$  remained constant. In their analysis of aquifer transmissivity ( $T$ ) from field tests, Sanchezvila et al.<sup>98</sup> indicated the departure from a traditional stochastic approach, when transmissivity is treated as a multilog-normal random function with a large-scale effective  $T$  equal to the geometric average of local measurements. Sanchezvila et al.<sup>98</sup> also found that large-scale  $T$  appeared to be larger than the geometric average of local tests, and suggested that the scale dependence of  $T$  could partially result from the presence of high permeability zones that were better connected than average or low permeability zones. The presence of high permeability zones and rock anisotropy could also explain the results of Nimmo,<sup>99</sup>

who determined no particular relationship for the groundwater velocity on a scale from a meter to a kilometer. Furthermore, the traditional concept of scaling can also fail if different field methods are used at different scales.<sup>100</sup>

## 2. Unsaturated Soils

There are two categories of scaling techniques for modeling unsaturated water flow processes:<sup>6</sup>

1. *Physically based techniques*, based on dimensional and inspectional analyses, enable the conversion of physically interrelated dimensional parameters into nondimensional parameters that sustain the original interrelationship.<sup>101</sup>
2. *Empirically based techniques*, based on a functional-normalization technique, enable derivation of scale factors by using a least-square regression analysis of the system properties.

A variety of applications of scaling to soil science problems is discussed by Sposito,<sup>5</sup> Warrick et al.,<sup>102</sup> Russo and Bresler,<sup>103</sup> Liu and Molz,<sup>109</sup> and Sposito and Jury.<sup>105</sup> Scaling for unsaturated flow is based on two main approaches: a similitude analysis of Richards' equation<sup>5</sup> and a similitude analysis of unsaturated hydraulic parameters — water retention and unsaturated hydraulic conductivity functions.<sup>106</sup> The original Miller and Miller<sup>106</sup> concept of scaling is based on using the scale factor  $\lambda$  to adjust the degree of magnification or reduction of the unsaturated hydraulic conductivity,  $K_i(\Theta)$ , and water potential,  $P(\Theta)$ , relative to a standard (reference) value. This concept is based on the assumption of geometrically similar (Miller-similar) porous media. In each local region of the formation, the scaled functions are supposed to be exactly the same and are expressed by either power law or exponential functions. The Miller-Miller scaling relationships are given by

$$\Theta^* = \Theta, P^* = \lambda P \text{ and } K^*(P^*) = (1/\lambda^2) K(\lambda P) \quad (20.3)$$

where  $\Theta^*$ ,  $P^*$  and  $K^*$  are the reference (scaled) values of the moisture content, water pressure, and hydraulic conductivity. For a known scaling factor the hydraulic properties at all locations can be calculated from the reference values of  $K$  and  $P$  determined at a reference region.

Warrick<sup>102</sup> and Warrick and Nielsen<sup>107</sup> proposed a generalization of the Miller-Miller similitude that considered the spatial variability of soil water properties at a field scale. Using a field-wide mean Richards' equation with field-scale averaged hydraulic parameters, a set of scaling factors is given by:<sup>108</sup>

$$\begin{aligned} S_m &= S_i^b \\ P_m &= \alpha_i P_i \\ K_m &= K_i / \omega_i^2 \end{aligned} \quad (20.4)$$

where  $S$  is the saturation,  $S = (\Theta - \Theta_r) / (\Theta_s - \Theta_r)$ ,  $\Theta_s$  and  $\Theta_r$  are the saturated and residual water contents, symbol  $m$  denotes a field-wide average, and  $i$  denotes a specific location. Sposito,<sup>5</sup> who reported a summary of several attempts to find the correlation between different scaling factors, showed that for different soils and types of experiments, these correlations may or may not be found. The Richards equation can also be written in a dimensionless form with only two types of parameters: the reference hydraulic properties and the scaling factor.<sup>109</sup>

Thus, according to the Miller-Miller approach, the volumetric water content does not vary with scale (i.e., scale invariant), and water potential and hydraulic conductivity are scaled with a single scale factor for length. According to the Warrick approach, the relative saturation is scale invariant,

and the water potential and hydraulic conductivity are scaled using different dimensionless scale factors. By comparing several examples of water retention functions, Sposito<sup>5</sup> concluded that scale invariance is a more general concept than that of fractal self-similarity<sup>110,111</sup> and that fractal models for the same porous medium are not equivalent.

In studying the invariance of Richards' equation subject to length- and time-scaling transformations, Sposito<sup>5</sup> and Sposito and Jury<sup>105</sup> found that a scale-invariant Richards' equation for any homogeneous domain (within a heterogeneous field) or for the entire soil formation (using averaged parameters) must hold if

- Hydraulic conductivity,  $K(\Theta)$ , is a power-law or an exponential function of the volumetric water content,  $\Theta$ .
- Relative saturation,  $S$ , is the scale invariant with a power-law relationship  $S(P)$ .
- Soil hydraulic properties are related to each other based on the Warick-Neilsen scale parameters  $\alpha_i$  and  $\omega_i$ .

The symmetry of Richards' equation under scaling is supposed to be broken if the scaling is applied only to the water content and the time variables, with no scaling of the water potential.<sup>5</sup> After solving Richards' equation with field-wide mean parameters for a given set of boundary and initial conditions, the specific parameters at a location  $i$  can be determined, if scaling parameters are known.

Based on the solution of Richards' equation and using Philip's solution for the cumulative infiltration rate into a soil column, Haverkamp et al.<sup>6</sup> showed that, theoretically, there is no unique dynamic similarity for soil water behavior, except for particular cases of the Green-Ampt and Gardner soils. However, from the practical standpoint, the similarity hypothesis is an adequate approximation. Haverkamp et al.<sup>6</sup> expressed the basic scale factors (for the saturation, pressure, and unsaturated hydraulic conductivity) as functions of the initial and boundary conditions, types of soils, and the space and time scale factors.

To simulate the area-averaged flow characteristics, Dagan and Bresler<sup>112</sup> assumed that (1) the soil is a set of locally homogeneous columns through which water moves by gravity, and (2) the scaling factor is distributed log normally. They determined vertical one-dimensional water flux,  $q_i$ , at location  $i$  from

$$q_i = \alpha_i^2 K_{sat}^* (\Theta_i / \Theta_{sat})^{1/\beta} \quad \text{for } q_i < K_{i,sat}^* \quad (20.5)$$

where  $\beta$  is a constant,  $K_{sat}^*$  is the reference value of the saturated hydraulic conductivity,  $\Theta_i$  is the moisture content in the region  $i$ , and  $\Theta_{sat}$  is the saturated moisture content (or porosity).

However, field soil heterogeneity precludes using a single value for the scaling factor. Jury et al.<sup>113</sup> used two scaling factors and showed that no single scaling factor can remove the variability from the field data. Moreover, the variance and mean values of scaling factors for the functions  $K(S)$  and  $P(S)$  may be different.<sup>114</sup>

### 3. Unsaturated Fractured Media

Tidwell and Wilson<sup>115</sup> described the results of laboratory measurements of gas permeability on a relatively homogeneous block of Berea sandstone, and found that air-permeability measurements made at four discrete sample supports exhibit strong, consistent trends in the mean, variance, and semivariogram as a function of sample support. Bodvarsson et al.<sup>7</sup> presented the results of laboratory and field air-injection tests conducted to determine air permeability of fractured tuff at different scales at Yucca Mountain. Figure 20.3a demonstrates the types of tests, and Figure 20.3b shows that the scale-variation of air permeability can be described using Equation 20.2. We explain a possibility of scaling for air permeability in dry unsaturated rocks by the fact that air flow in rock

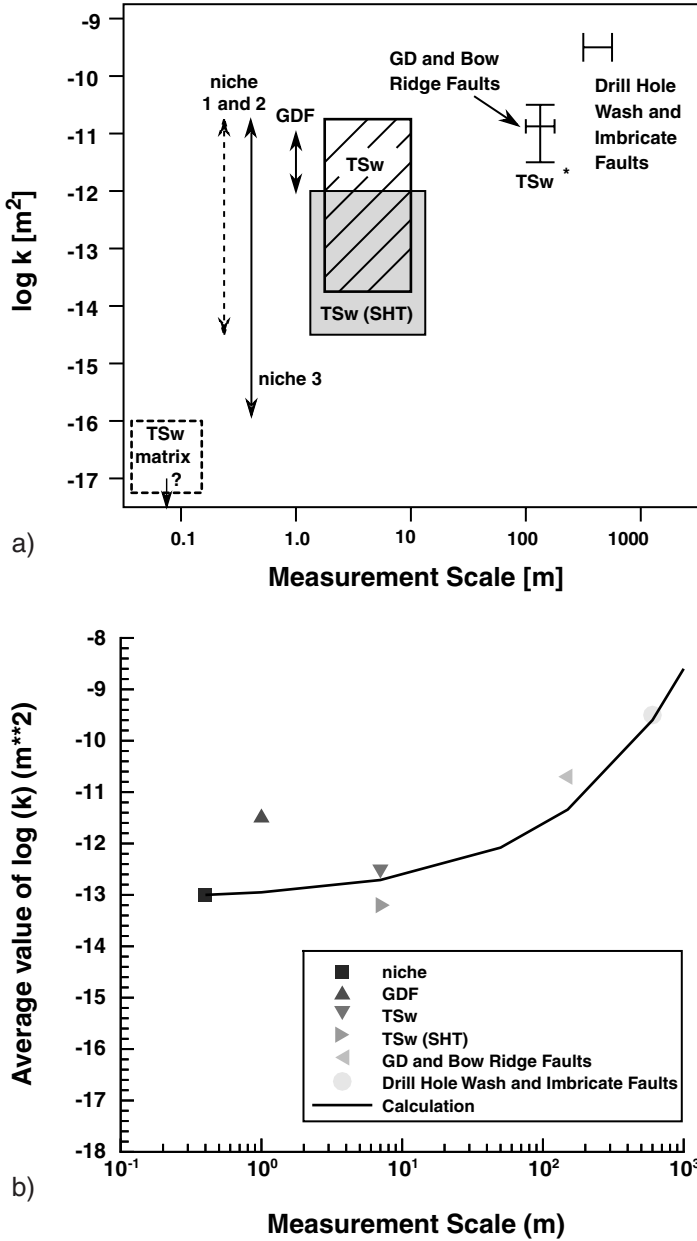


**FIGURE 20.3** Illustration of the types of tests and the ranges of permeability (upper panel) and the results of the determination of rock permeability (lower panel), using air-injection tests at different scales at Yucca Mountain, demonstrating the validity of the scaling relationship (20.2). (From Bodvarsson, G.S. et al., in *Conceptual Models of Flow and Transport in the Fractured Vadose Zone*, National Academy Press, 335, 2001. With permission.)

is supposedly taking place in continuous (but heterogeneous) media with the same physics of flow and geometrical similarity at different scales.

Scale effects for unsaturated flow processes are expected to be more complicated than those for saturated media because the assumption of the same physics of flow and geometrical similarity may not be applicable to unsaturated fractured rocks. It is apparent that no scaling for water pressure or moisture content can be made for flow processes in fractures and matrix because of different physical

flow processes in these two domains of fractured rock. Therefore, scaling assumptions developed for unsaturated porous media are likely to be invalid for water flow in unsaturated fractured rock. This may explain the results of Clauser,<sup>17</sup> who did not observe scaling of permeability in fractured rock.

Different nonlinear hydraulic processes are governing flow in fractured rocks on different scales. Moreover, the scale of measurements in the vadose zone (using point-type, near-borehole, and cross-borehole measurements) is inconsistent with the scale of flow processes in the field. For example, hydraulic conductivity increases or decreases depending on sample size.<sup>116</sup> Heffer and Koutsabeloulis<sup>117</sup> determined that despite the presence of a scaling relationship for the fracture frequency and the fracture trace lengths from single cores to thousands of meters, the scaling of hydraulic properties determined for small dimensions cannot be applied to the larger dimensions.

Complex flow behavior in fractures leads to departure from the cubic law for flow — even in a single fracture.<sup>116</sup> The main factors affecting flow are aperture distribution, changes in the aperture distribution during deformation, and flow through a critical “neck.” Assuming a combination of these nonlinear factors, even granting the validity of the cubic law for flow on a local scale, a macroscopic flow rate yields an exponent much larger than cubic.<sup>116</sup> In general, the concept of scaling may not be valid for a dissipative system such as fractured rocks, because the macroscopic properties of the system are different at each hierarchical level of a system.<sup>118</sup>

## B. EFFECTIVE HYDRAULIC PARAMETERS FOR HETEROGENEOUS MEDIA

In heterogeneous porous and fractured media, many different flow processes influence each other within a certain volume of media, leading to an *intrinsic* volume averaging of the flow processes. In addition, the use of monitoring probes leads to an *extrinsic* volume averaging of flow processes in the vicinity of these probes. However, the volumes of intrinsic and extrinsic averaging may not coincide because the size of field probes is usually larger than the pore scale or a fracture aperture. Therefore, empirical models based on field measurements may have no direct relevance to real physical phenomena (in either pores or fractures) or to mathematical models of these processes.

The governing equations for fluid flow and transport in the subsurface are usually written using macroscopic, volume-averaged (integrated over a certain volume of media) or time-averaged (integrated over a certain time interval) properties.<sup>119</sup> These properties are often called the effective parameters of media. Effective parameters are used to derive empirical models directly from measurements of the variables of interest, without considering the relationship between these variables on scales smaller than the scale of measurement.<sup>5</sup> If the scale of measurements is sufficiently small, spatial variations in measured soil and rock properties lead to a spatial heterogeneity of flow parameters.

Flow in fractured rock is significantly affected by the complexity of fracture networks and fracture–matrix interactions, which makes the task of precisely describing flow processes using basic pore-scale equations practically impossible.<sup>120</sup> Using measurements, we aggregate pore-scale flow processes so that measured volume-averaged variables vary smoothly over the field scale. These variables can then be used to describe flow processes using differential equations with parameters, which are likely to be different for different scales. As the volume of measurements increases, the spatial variation of flow parameters decreases, reducing the degree of apparent heterogeneity in the flow field.

The volume of media within which flow parameters are averaged and remain practically constant is called a representative elementary volume (REV). REV describes the general concept of identifying the cut-off size for treating a medium as homogeneous.<sup>121</sup> As the measurement volume increases, flow variables may become significantly different (either larger or smaller), indicating the departure from a continuity hypothesis. In practice, the REV is a hypothesis, according to which the experimentally measured variables are presented as parameters (quantities) in flow equations. Thus the following questions arise: “What is the real physical meaning of this mathematical quantity?” and “What quantity does one ideally wish to measure?”<sup>122</sup> In hydrology, the REV concept

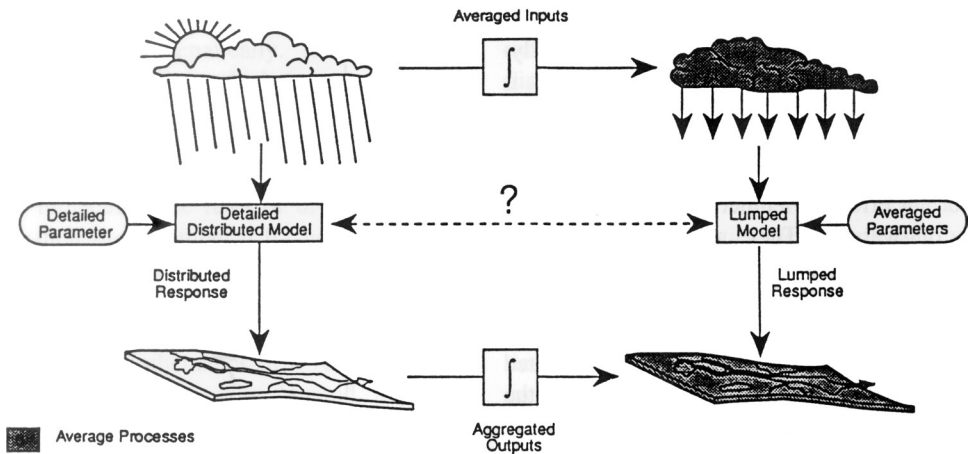


**FIGURE 20.4** Schematics of distributed and lumped models for simulations of hydrogeologic processes. (From Wood, E.F., in *Scale Dependence and Scale Invariance in Hydrology*, Sposito, G., Ed., Cambridge University Press, Cambridge, 1, 1998. With permission.)

is identical to that originally developed in the field of continuum mechanics to describe macroscopic properties of gas or liquid (e.g., velocity, temperature) by averaging over a large number of molecules. These properties are then used to formulate the equations of motion on a continuum basis.<sup>122–124</sup> A continuum approach for heterogeneous media can be considered for conditions of large-scale correlation and fluid-phase connectivity.<sup>125</sup>

REV has become the subject of much debate, because the main goal of defining an REV scale is to justify the use of empirical models developed at the macroscopic (measurement) scale.<sup>126,127</sup> For example, Yeh<sup>120</sup> indicated that the size of REV is scale dependent, so the REV identified for a laboratory experiment may not be applicable for a field-scale problem. Yeh also indicated that the aggregation of field-scale heterogeneities using large-scale field experiments generates fictitious hydraulic properties. The assumption of stationarity is another drawback of the REV hypothesis.<sup>120</sup> Neuman<sup>128</sup> stated that “there is generally no guarantee that an REV can be defined for a given rock mass. When an REV can be defined, it is often so large as to render the measurements of its hydraulic conductivity impractical.”

Figure 20.4 demonstrates in general how to use a distributed model, which considers explicitly the variability of parameters, and a lumped model (with averaged parameters), which does not consider spatial variability, i.e., a single column model, for hydrologic investigations. The main question that arises is: what is the limit of application for the upscaling model (or averaging), so that the results of using both models are the same? Wood<sup>129</sup> found that as nonlinearity in the point-scale processes increases, the application of two models would generate significantly different results.

### C. HIERARCHY APPROACH

Hierarchy theory is used to provide an ordered ranking of a system’s components, assuming that a system consists of several components.<sup>26,118</sup> Figure 20.5 presents a schematic of a hierarchy of graded or ranked system components, with each component dominant over those below it and dependent on those above it. Using this hierarchical structure, the system components are coupled with vertical connections (connecting separate hierarchical levels) and horizontal connections (connecting system components on the same hierarchical level). These connections present the type of loose coupling that allows the investigator to decompose the system to study separate components while preserving the inherent interaction between components, which, in turn, determine the collective behavior of the hierarchical system.

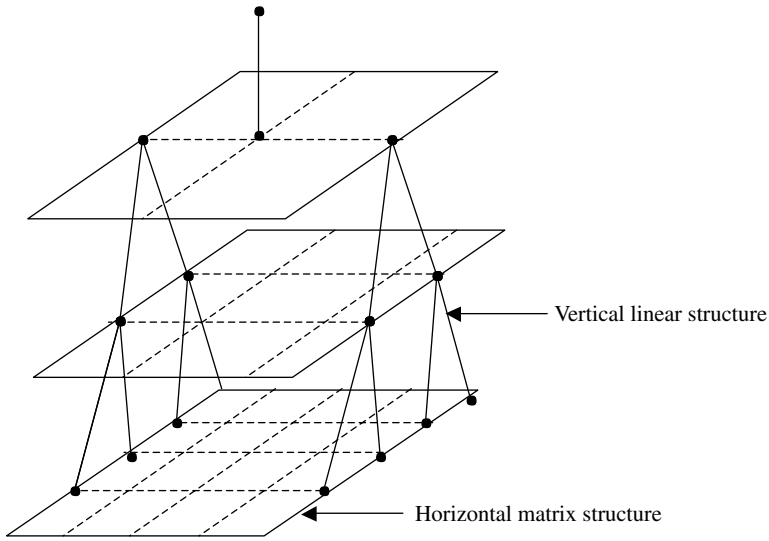


**FIGURE 20.5** Illustration of a concept of a hierarchy of scales, showing a system structure of a graded (ranked) series of system parts (subsystems) with vertical (linear) and horizontal (matrix) connections, with each subsystem dominant over those below it and submissive to those above it.

Wagenet and Hutson<sup>29</sup> presented an 11-level hierarchy of scales for soil-science investigations shown in Figure 20.6. In this hierarchy, the main level of interest is a pedon (the Greek word *pedon* means a layer of soils), which is defined as a three-dimensional natural body of soils that is large enough to represent natural conditions and variability of soil horizons.

To describe a process effectively, using a hierarchy of scales requires a minimum of three levels (a triadic structure).<sup>26</sup> Assuming that the hierarchical level of interest is called Level 0, a hierarchy should include at least one hierarchical level above it, called Level +1, and at least one hierarchical level below it, called Level -1 (Figure 20.7). The characteristics of the lower-level components can

### Hierarchy of Spatial Scales of Solute Transport Models

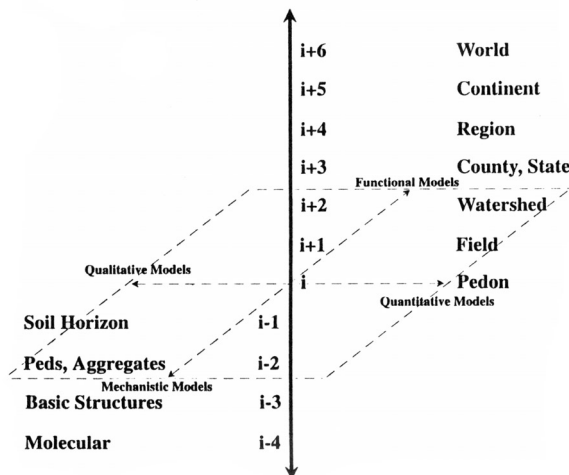


**FIGURE 20.6** Eleven- level hierarchy of scales for soil science investigations. (From Wagenet R.J. and Hutson, J.L., *J. Environ. Qual.*, 25(3), 499, 1996.)

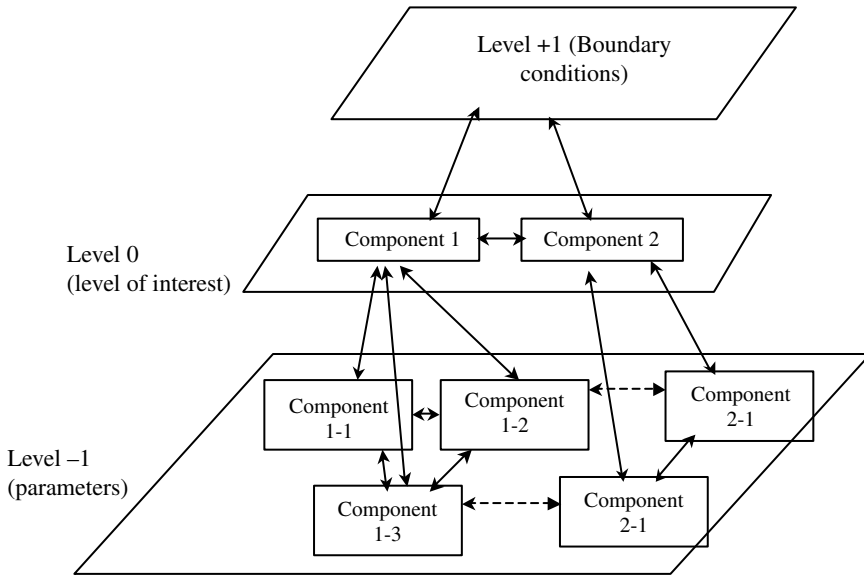


**FIGURE 20.7** Illustration of the triadic hierarchical structure: the dynamics of Level 0 (the level of interest) are affected by the interaction of its components on Level -1 (used to determine parameters), and are constrained by the dynamics of processes on a higher level: Level +1 (used to determine boundary conditions).

be considered as state variables of a higher level, so that Level -1 characteristics are state variables for Level 0, and Level 0 characteristics are state variables for Level +1. Level -1 is used to describe in detail the dynamics at the background level of the system. The interaction among components of Level -1 determines the range of processes at Level 0. The low-frequency behavior at Level +1, which constrains the higher-frequency dynamics of Level 0, determines the system boundary condition within which the system is expected to behave over time.

Thus, for such a hierarchical organization, the smaller-scale dynamics on Level -1 are integrated into the larger-scale dynamics of Level 0, and the smaller-scale dynamics on Level 0 are integrated into the larger-scale dynamics of Level +1. The dynamics of processes on Level 0 depend on processes occurring on the higher and the lower scales of the hierarchy. The processes on the levels higher than +1 can be considered too slow to affect Level 0, whereas the processes on levels below -1 are too noisy compared to fluctuations on Level -1.

The overall dynamics of the processes on higher levels may appear constant over a period of observation. At the same time, the processes on the higher level may serve as forcing (driving) variables for those on lower levels. For example, ambient conditions (precipitation, temperature, barometric pressure), as well as the depth and range of water table fluctuations, predetermine the range of flow rate and moisture content in the vadose zone. The drastic variations of atmospheric conditions (catastrophic events) may perturb the system so that monitoring the recovery would indicate the transition rate to a quasi-stable state and may be used to assess the system's stability.

## IV. EXAMPLES OF INVESTIGATIONS OF FRACTURED ROCK

### A. FRACTURED BASALT OF THE SNAKE RIVER PLAIN, IDAHO

#### 1. Geologic Conditions

The Snake River Plain is primarily composed of fractured Quaternary basalt flow units, interlayered with sedimentary deposits.<sup>130,131</sup> The thickness of these deposits varies from a few centimeters to as much as 15 m. Basalt flow units comprise a number of basalt flows arising from the same

eruption event. Individual basalt flows generally consist of multiple lobes elongated in one direction, giving them a finger-like or lenticular structure. Typical lobe dimensions are 3 to 12 m thick and 20 to 60 m wide, with lengths of up to 1 km.<sup>130</sup> Geophysical logging and borehole coring results suggest that the total basalt thickness in the Snake River Plain may exceed 3 km.

Basalt flows are typically highly fractured or rubbled at the flow margins. The discontinuities that affect water flow the most in fractured basalt are column-bounding fractures (also called joints),<sup>132,133</sup> intrabasalt fractures, fracture zones, and rubble zones. Column-bounding fractures in basalt usually form a polygonal network created perpendicular to the cooling isotherm because of thermal contraction in basalt lava. Near the upper surface of the basalt flow, the spacing between fractures is as low as 0.3 m. The spacing between fractures increases with depth within the upper two-thirds of the flow thickness. The lower one-third of the basalt flow shows an inverted pattern, with a narrow spacing at the base of the flow that widens upward towards the center of the flow. In some basalt flows, the center of the basalt flow contains highly fractured rock with no columnar fracturing.<sup>134</sup> The porosity of the basalt matrix, determined from core samples by Knutson et al.,<sup>130</sup> ranges from 20 to 40% with an arithmetic mean of 19.2%. The geometric mean permeability for the basalt matrix is  $2.24 \times 10^{-15} \text{ m}^2$  and for the vesicular zones it is  $10^{-12} \text{ m}^2$ .

## 2. Hierarchical Scales for Fractured Basalt

The concept of a hierarchy of investigations for fractured rocks is based on the assumption of a four-level hierarchy of hydrogeological components, including elemental-, small-, intermediate-, and large-scale components.<sup>32</sup> The relationship among these components is illustrated in Figure 20.8. Elemental-scale investigations are conducted under laboratory or field conditions, whereas small-, intermediate-, and large-scale investigations are conducted exclusively under field conditions. Based on the concept of triadic structure described in Section III.C.1, Table 20.1 shows the linkage between levels of investigations for four scenarios, depending on what is chosen for Level

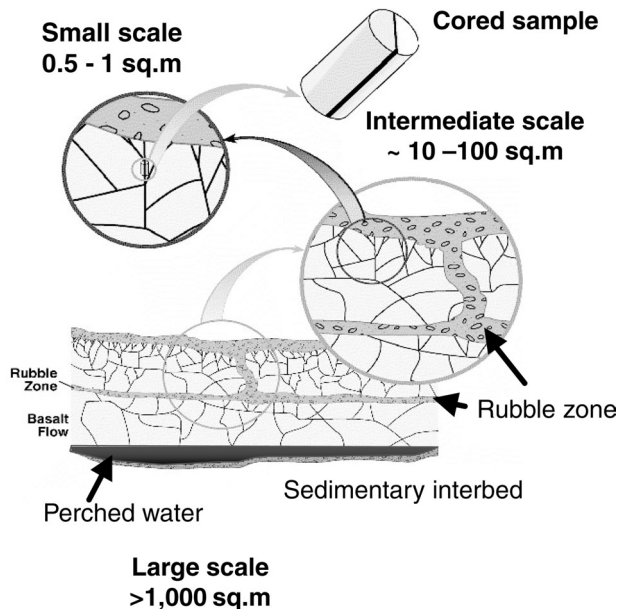


**FIGURE 20.8** (See color insert following page 144.) Illustration of a hierarchy of scales for fractured basalt. (From Faybishenko, B. et al., in *Flow and Transport through Unsaturated Fractured Rock*, Geophysical Monograph No. 42, 2nd Ed., Evans, D.D., Nicholson, T.J., and Rasmussen, T., Eds., 161, Published 2001 American Geophysical Union. With permission.)

**TABLE 20.1**  
**Linking Hierarchical Scales of Investigations**

Types of investigations	Hierarchical scales	Levels			
Laboratory	Elemental scale — core testing	Level -1 (infracrature and intramatrix measurements)			
Field scale	Small scale	Level 0 Level +1 (boundary conditions according to the regime of fluctuations)	Level -1 Level 0	Level -1	Level -1
	Intermediate scale		Level +1	Level 0	
	Large scale			Level +1	Level 0 Level +1 (watershed and atmospheric processes)

0: elemental-, small-, intermediate-, or large-scale components. For each of the four scenarios, an investigation on Level 0 involves monitoring/measurements on Level -1 and an assignment of boundary conditions on Level +1.

*Elemental scale components* of fractured basalt include a single fracture or a block of porous media (matrix). The size of the elemental component ranges from a few centimeters to 10 to 20 cm. Elemental components can be studied using small laboratory cores, fracture replicas, or miniature-sized probes under field conditions. Results of experiments on this scale can be used to describe, in detail, specific flow and transport processes in fractures, matrix, or fracture–matrix interactions. Some examples of these flow processes are: (1) water dripping from a fracture under field conditions in boreholes, tunnels, caves, or other underground openings; (2) film flow<sup>66</sup> and water meandering along a fracture surface in laboratory experiments;<sup>51</sup> and (3) water dripping within flow channels, or intermittent flow, along a fracture surface in laboratory experiments.<sup>52</sup> For an experiment conducted on a single core, Level -1 measurements are performed to determine the fracture aperture distribution, temporal fluctuations of liquid and gas pressure, water dripping, the area covered by water, and fracture–matrix interaction. Level +1 boundary conditions are assigned to simulate the expected changes in the flow regime on a small or intermediate scale.

*Small-scale components* include a volume of rock within a single basalt flow with one or a few fractures. The areal extent of small-scale components is approximately 0.5 to 1 m<sup>2</sup>. Results of field experiments on this scale can be used to describe in detail some of the flow and transport processes in one or a few intersecting fractures.<sup>63</sup> Small-scale infiltration experiments are conducted to investigate fracture–matrix interaction, dripping-water phenomena, and small-scale averaging of flow rates and water pressures measured in fractures and matrix. Field measurements (Level -1) are performed to determine a single fracture location or a fracture pattern, flow rate, water and gas pressure, tracer concentration, or moisture content in a fracture or matrix (the probes may intersect fractures and matrix). Geophysical (single- and cross-borehole) methods can be used to assess water distribution. Boundary conditions (Level +1) are usually assigned to simulate infiltration caused by water ponding, episodic precipitation, irrigation, or temperature regime changes.

*Intermediate-scale (mesoscale) components* include a volume of rock within a basalt flow involving all types of fractures, such as the fractured flow top, vesicular or massive basalt, fracture zones in the upper and lower fractured colonnade, and the central fractured zone or entablature, fractured flow bottom, and fractures intersecting the basalt flow and rubble zone.<sup>50</sup> The areal extent of intermediate-scale components is approximately 10 to 100 m<sup>2</sup>. The results of field experiments at this scale can be used to describe volume-averaged flow and transport processes within a single basalt flow. Mapping of a fracture pattern is required to assess the overall geometry of flow. Boundary conditions (Level +1) depend on relief/topography and permeability of the topsoil layer, which determines the redistribution of water on the ground surface, including surface runoff and infiltration. Boundary conditions (Level +1) are assigned (as for a small scale) to simulate infiltration as a result of such events as water ponding, episodic precipitation, irrigation, or temperature regime changes. Field measurements (Level -1) are essentially the same as those for small- and intermediate-scale field investigations, but involve a larger number of probes, thus increasing the volume of rock and intersecting real boundaries (discontinuities).

*Large-scale (regional) components* involve a volume of rock containing several basalt flows and the rubble zones between them. The areal extent of a large-scale component usually exceeds 1000 m<sup>2</sup>. At this scale, one can study flow in the fracture networks and regional hydrogeological processes, which are affected by the network of vertical and horizontal rubble zones as well as sedimentary interbeds. Because the flow processes occurring on the intermediate and large scale are greatly influenced by atmospheric processes, measurements of meteorological conditions are an essential part of large-scale investigations.<sup>135</sup>

Atmospheric processes (precipitation, humidity, and pressure) present a higher-level constraint for the hydrogeologic processes that, in turn, control ambient conditions resulting from evapotranspiration. For example, air humidity is affected by moisture released through evapotranspiration, while evapotranspiration dynamics are a function of precipitation and ambient temperature. Vegetation appears as a state variable of the precipitation model, and precipitation appears as a state variable of the vegetation model. The state variables describing large hydrological systems may change on different time scales according to the variability of atmospheric processes — seasonal, annual, and decadal. (Rapid temporal changes in small-scale hydrologic systems and slow changes in large systems can be counter to atmospheric systems that may behave quite rapidly on large spatial scales or small temporal scales.) The dynamics of large-scale hydrological systems are not considered for small time scales. When the spatial level of a hierarchy increases, the overall time duration of monitoring increases.<sup>136</sup> Hierarchy of scales can be used to optimize investigations by finding a coherent correspondence between space and time scales for the hydrologic system. For a hydrologic system, as discussed below in Section IV.A.3, the total inflow rate constrains the outflow rate, and the outflow is, in turn, a feedback for the infiltration rate.

### 3. Infiltration Tests on a Hierarchy of Scales

#### a. Types of Tests

The results of water-flow investigations in fractured basalt are illustrated below, using the results of three ponded infiltration tests carried out at three different sites:

1. *Small-scale* infiltration tests conducted at the Hell's Half Acre (HHA) site near Idaho National Engineering and Environmental Laboratory (INEEL), with water supplied from an infiltration gallery of  $0.5 \times 1 \text{ m} = 0.5 \text{ m}^2$  and water collected in 12 collection trays, each of  $0.2 \times 0.2 \text{ m} = 0.04 \text{ m}^2$  on the underside of the basalt column, with a  $0.48 \text{ m}^2$  collection tray area<sup>63</sup>

2. *Intermediate-scale* infiltration tests conducted at the Box Canyon (BC) site at the scale of  $7 \times 8 \text{ m} = 56 \text{ m}^2$ , with nine infiltrometers 20 cm in diameter (area  $0.031 \text{ m}^2$ ) installed within the infiltration pond<sup>50</sup>
3. *Large-scale* infiltration test (LSIT) conducted at the Radioactive Waste Management Complex, using a pond of 200 m in diameter ( $31,416 \text{ m}^2$  in area)<sup>137,138</sup>

### b. Variations of Infiltration Rates for Different Scales

Measurements of the infiltration rate conducted at the small-scale HHA<sup>63</sup> and the intermediate-scale BC sites<sup>50</sup> confirmed the presence of spatial and temporal variations in the flow rate. At the HHA site, temporal variations in the infiltration and outflow rates<sup>63</sup> exhibited a general three-stage pattern identical to that observed in laboratory and field tests for soils in the presence of entrapped air.<sup>48,49</sup> The HHA tests conducted under nearly the same boundary conditions are not exactly repeatable, but the identical three-stage temporal pattern of the flow rate can be observed. Despite constant water-head boundary conditions in the supply reservoir at the surface, infiltration and outflow rates did not achieve steady state for up to 18 days. The HHA tests confirmed that the small-scale flow dynamics might change drastically as new fractures or flow channels are opened for flow, causing the flow geometry to change. A particular fracture may serve as a capillary barrier blocking water flow until the water pressure falls below a critical value, and the same fracture may become a water conduit, causing a drastic increase in flow rate, once water pressure exceeds a critical value.

Small-scale infiltration tests conducted at the HHA site showed an extensive variety of patterns for infiltration and outflow rates, as well as water dripping at several locations from a single fracture. All these phenomena were unstable and irregular in space and time, even under a constant ponded-water level at the surface.<sup>63</sup> The nonlinear-dynamics analysis of the flow rate and the frequency of dripping water revealed nonperiodic, chaotic behavior for an intrafracture flow and a capillary-barrier effect at the exit of a fracture, which can be described by a Kuramoto-Sivashinsky equation (see Section V.B). One of the most important features observed from these infiltration tests is the complex relationship (feedback) between inflow (at the surface) and outflow (at the underside of the basalt column) rates. For example, if the fracture serves as a capillary barrier, the infiltration rate is restricted to flow (vertical and backward) through the matrix. Once a fracture becomes a flow-through conduit, the increase in the outflow rate causes an increase in the infiltration rate.

Figure 20.9a shows a comparison of the temporal variations in the infiltration rates recorded at Box Canyon<sup>50</sup> and HHA<sup>63</sup> infiltration tests. The increase in flow rate, which began at the small-scale HHA site 2 to 4 days after the beginning of infiltration, was not evident during a series of intermediate-scale tests at the BC site. Figure 20.9b illustrates a drastic difference in flow rates measured in several trays installed on the underside of the basalt column at the HHA site. The higher HHA infiltration rates in comparison with those in the BC tests could be explained by the fact that the topsoil layer was removed from the HHA and a fracture was exposed at the surface, whereas topsoil partially covered the BC site. Infiltration is likely to cause soil particles to penetrate into the near-surface fractures, seal some of the fractures, and decrease the temporal fluctuations in the infiltration rate, leading to a narrow range in the final rates.

Figure 20.10 summarizes the ranges of infiltration flux (essentially the same as the rock hydraulic conductivity) for the HHA, Box Canyon, and LSIT sites conducted over the area ( $0.03$  to  $31,416 \text{ m}^2$ ). This figure shows that the infiltration rates at the LSIT and the BC tests are within the range of the rates for the HHA site. We may assume that as the scale of the test increases, the variations in infiltration rates decrease and the flow rate over the area of the pond is averaged, with no scaling relationship evident from experimental data. (A low value of infiltration rate for the LSIT site can be explained by sealing near-surface fractures, and the fact that the interbasalt-flow rubble zones are sealed with relatively low-permeability soils.) The analysis of variations of field-determined permeability supports one of the concepts of the hierarchy theory — that the system components at lower levels fluctuate at higher rates than those at higher levels.

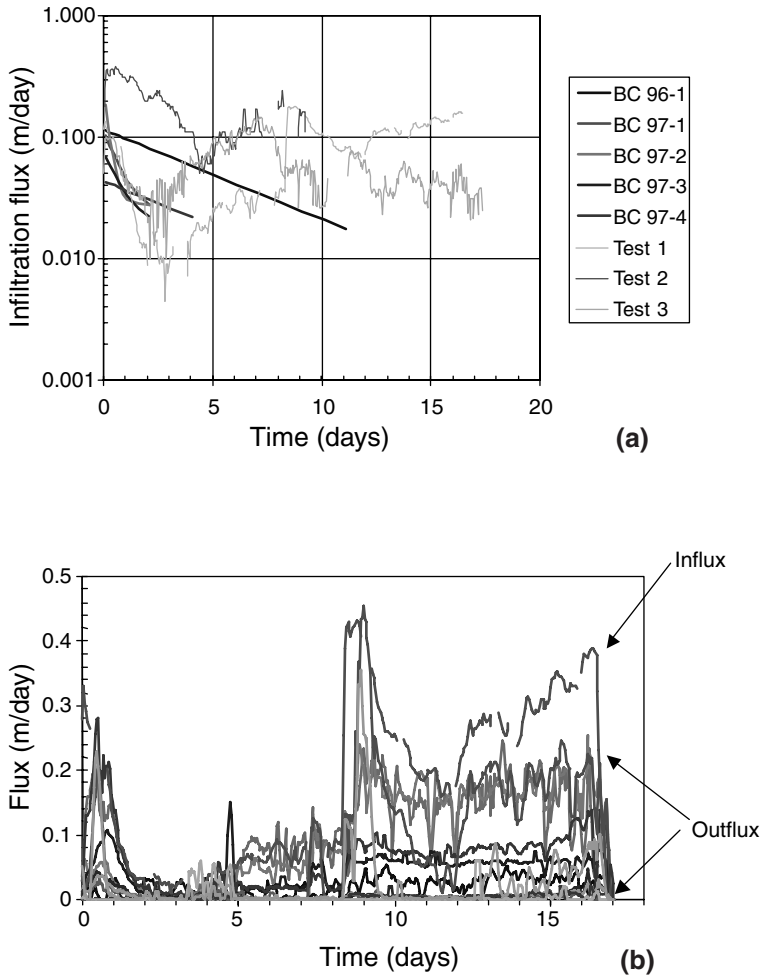


**FIGURE 20.9** (See color insert following page 144.) (a) Comparison of Box Canyon (BC 96–1, BC 97–1, BC 97–2, BC 97–3, and BC 97–4) and HHA infiltration rates (Tests 1 through 3), and (b) comparison of HHA infiltration and local outflow rates measured in separate trays ( $20 \times 20$  cm) for Test 1. HHA data are from Podgorney, R. et al., in *Geophysical Monograph No. 122: Dynamics of Fluids in Fractured Rock*, Faybishenko, B., Witherspoon, P.A., and Benson, S.M., Eds., 129, 2000. American Geophysical Union. (Figure 20.9b reproduced by permission of American Geophysical Union.)

Numerical modeling of Box Canyon tests showed that the infiltration rate may increase with time as the middle basalt flow fractures become saturated.<sup>139</sup> The same range of temporal and spatial variations for infiltration rate suggests that the ergodicity hypothesis (ensemble average equal to time average) is applicable to fractured basalt. Different temporal behavior of the infiltration rate at different scales (affected by fracture–matrix interaction, fracture sealing, and entrapped air redistribution) is indicative of processes taking place on a hierarchy of scales. The data also confirm that small-scale infiltration-rate fluctuations of inflow rate (occurring daily and affected by opening of the fractures) occur more rapidly than those at an intermediate scale. Comparison of the small-scale and intermediate-scale tests shows that the increase in flow rate observed at the HHA site was not observed at Box Canyon because the Box Canyon surface area was partially covered with soils. An HHA surface-exposed basalt was practically open. These tests also showed that rapid fluctuations in water pressure and small-scale flow rates are constrained by the trend of the total infiltration rate.

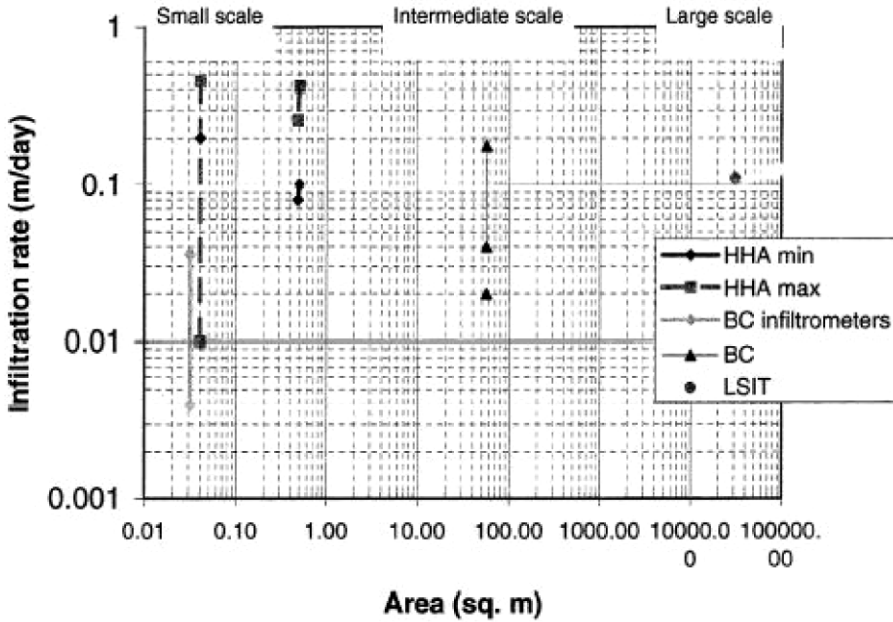


FIGURE 20.10 Ranges of the variation of infiltration rates vs. the ponded area in fractured basalt.

### c. Variations in Water Travel Time for Different Scales

Measurements (with tensiometers, suction lysimeters, and neutron probes) of the water arrival time during infiltration tests at HHA (to depth of 1 m), BC (to 20 m), and LSIT (to 55 m) are illustrated in Figure 20.11, and show the relationship between water arrival time and depth of the vadose zone. This figure demonstrates that the results of all infiltration tests at the three sites fall into two categories for the upper basalt flow:

1. Fast flow, which is likely to occur in fractures, at velocities on the order of 5 to 7 m/day or faster
2. Relatively slow flow, which is likely to occur through the matrix or low-conductive (or nonconductive) fractures

The distinct difference between these two flow categories provides clear evidence that fast flow in fractures can lead to bypassing in the rock matrix and nonconductive fractures. Relatively slow flow in the matrix can be caused by downward flow from the surface and water imbibition from conductive fractures. The high-permeability rubble zone between the upper and lower basalt flow serves as a hydraulic barrier for fast flow from the upper basalt flow, restricting fast downward flow and causing a lateral diversion of flow between basalt flows. As a result, the fast and slow flow patterns converge in the underlying basalt flow (Figure 20.11).

The relatively narrow ranges of water arrival times for the fast and slow flow categories can be explained by the resolution of small-size point-type (tensiometers, ER probes) or near-borehole (suction lysimeters, neutron logging) measurements being practically the same and independent of the scale of infiltration tests. These data also show that volume averaging of hydraulic properties over the field scale should be provided separately for the two distinct categories of fast and slow flow processes taking place in the upper basalt flow. Volume averaging for the underlying basalt flow could be provided by taking into account the cumulative effect of fractures and matrix. (Note that these findings arise from the results of infiltration tests that use a supply of ponding water at the land surface.)

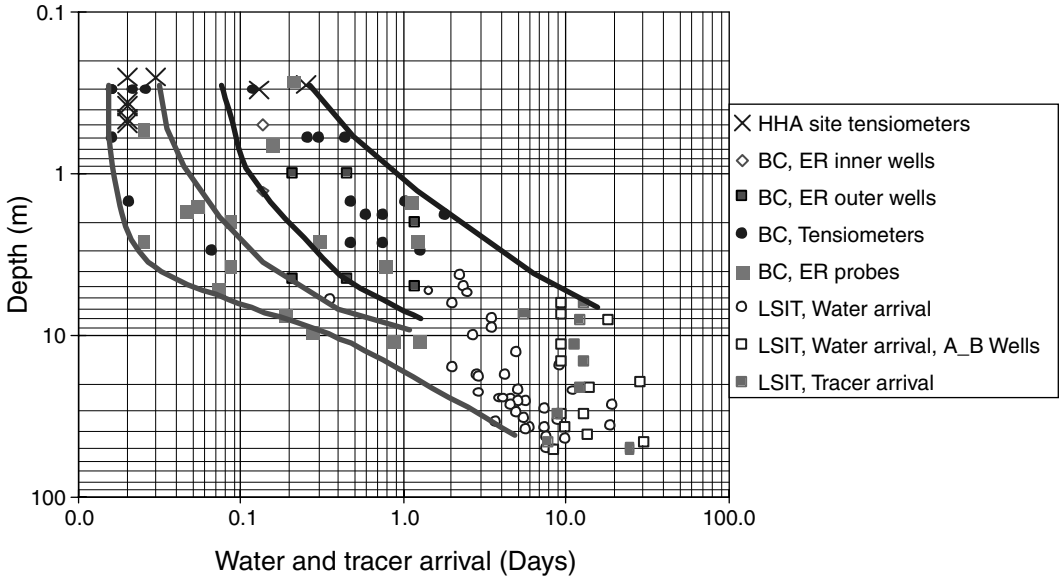


**FIGURE 20.11** Water arrival time with depth in fractured basalt under conditions of ponded infiltration. The data for the upper 1-m part of the vadose zone obtained at the HHA site are in agreement with those of 20-m depth Box Canyon tests. The Box Canyon data are in agreement with the results of the 55-m LSIT.

Thus, although the three ponded-infiltration tests demonstrated different mechanisms affecting flow processes and infiltration rates at different scales, the water travel time with depth in fractured basalt exhibited the same two distinct patterns. These patterns are typical for a double-porosity or double-permeability system, with some random variations around the averaged value caused by the heterogeneity of the fractures and matrix. For such a system, no scaling of a conventional Richards' equation is possible.

## B. FRACTURED TUFF AT YUCCA MOUNTAIN

### 1. Geologic Conditions and Types of Fracture Patterns

#### a. Location and Geologic Conditions

The high-level nuclear waste repository at Yucca Mountain, Nevada, is proposed to be located at a depth of approximately 300 m within a 600 m deep unsaturated zone.<sup>140–143</sup> The Yucca Mountain unsaturated zone consists of alternating sequential layers of variably fractured and faulted welded and nonwelded tuffs.<sup>144</sup> These tuffs have various geologic and hydrogeologic heterogeneities in the saturated and unsaturated zones, including stratigraphic heterogeneities, faults and associated offsets, dipping beds, and alteration zones, as well as perched-water zones. [Figure 20.12a](#) (central panel) presents a schematic cross section through Yucca Mountain, showing major subsurface layering and faults that are expected to affect flow and transport processes on the scale of hundreds of meters. According to Montazer and Wilson,<sup>145</sup> the geologic layers include (from the land surface downward): welded Tiva Canyon Tuff (TCw); mainly nonwelded rocks of the Paintbrush Group (PTn); welded Topopah Spring Tuff (TSw); mostly nonwelded and sometimes altered Calico Hills Formation (CHn); and mostly nonwelded and altered Crater Flat undifferentiated Group (Cfu). The proposed repository is to be located in the TSw unit within the following geological subunits: the middle nonlithophysal unit (10% of the repository), the lower lithophysal unit (80%), and the lower nonlithophysal unit (10%).

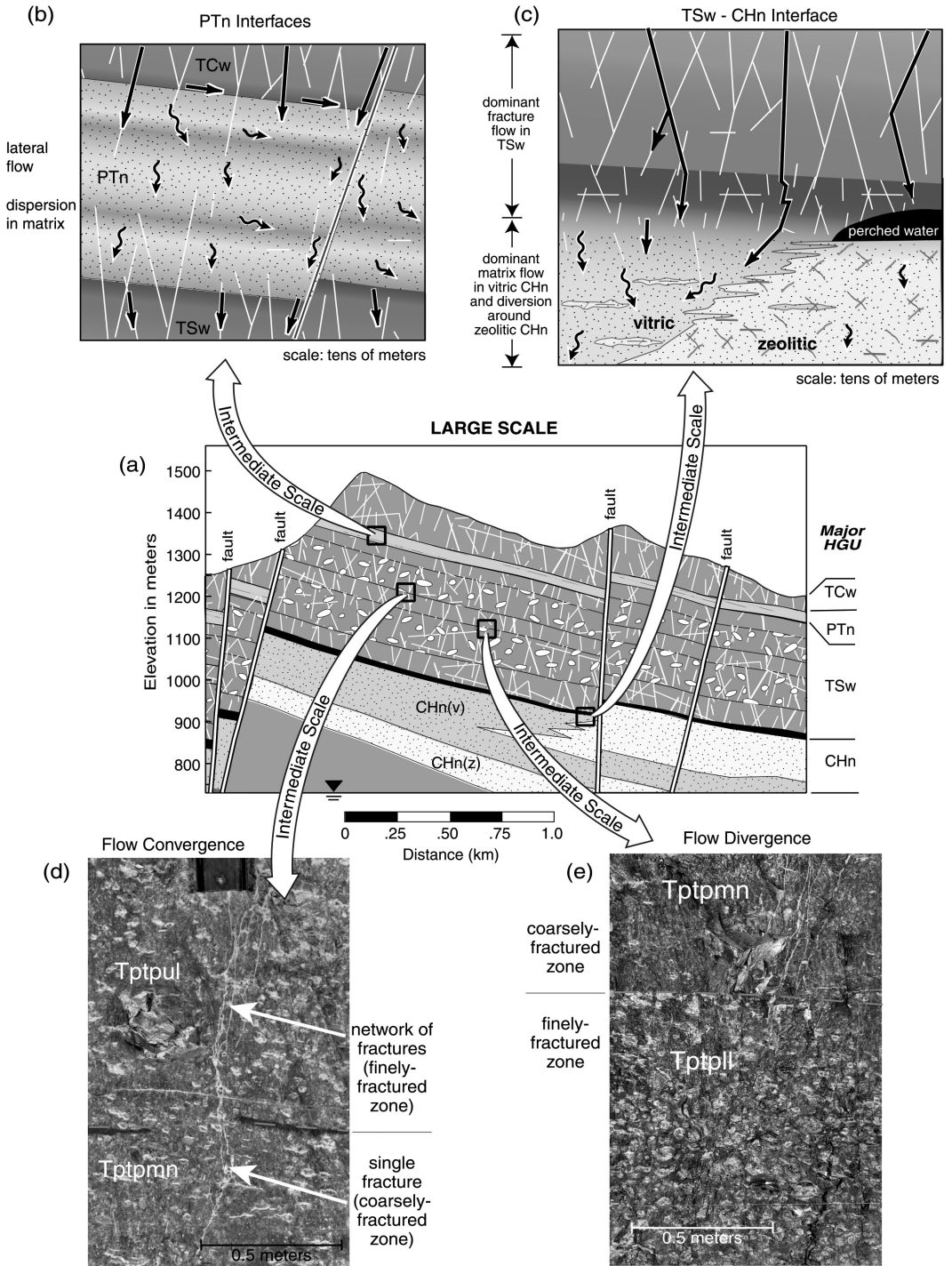


**FIGURE 20.12** Illustration of a general two-dimensional cross section through Yucca Mountain (central panel), showing several lithological units, representing a large-scale (site-scale) model, and examples of intermediate-scale flow processes typical for different lithological units (upper and lower panels). (From Bodvarsson, G.S. et al., *Unsaturated Zone Flow and Transport Model Process Model Report*, LBNL, 2000, and Bodvarsson, G.S., Bandurraga, T.M., and Wu, Y.S., *Technical Report LBNL-40378*, Lawrence Berkeley National Laboratory, 1997.)

*b. Fracture Characteristics*

Several papers have investigated the fractal properties of fractured tuff at Yucca Mountain.<sup>73,146,147</sup> Fractal analysis has also been used to predict the fractal structure and bypass flow in rocks.<sup>148,149</sup> According to Barton and Larsen,<sup>146</sup> who investigated the fractal geometry of two-dimensional fracture networks at three Yucca Mountain surface outcrops: (1) the distribution of fracture trace lengths is log normal, and (2) the network patterns are scale independent for trace lengths ranging from 0.2 to 25 m. For the same sites, La Pointe<sup>150</sup> determined that the fractal dimension of the fracture pattern ranged from 1.52 to 1.54, in contrast to the fractal dimension of rock blocks, which ranged from 2.37 to 2.69. Barton and Larsen<sup>146</sup> also suggested that the fractures do not form well-defined sets based on orientation, but Nieder-Westermann<sup>151</sup> suggested otherwise. Despite many investigations of the fractal properties of fracture networks, no simple relationship between a fractal dimension of the fracture network and rock permeability has been found.

To substantiate a possibility for using a hierarchical approach based on fracture characteristics, we analyzed the results of measurements carried out along the Exploratory Studies Facility (ESF) tunnel. We used the results of measurements taken 30 cm into the formation for the middle nonlithophysal TSw unit along the ESF (between Stations 10+80 and 37+80. Data were collected by Nieder-Westermann et al.), and plotted Figure in 20.13 to depict the relationship between fracture

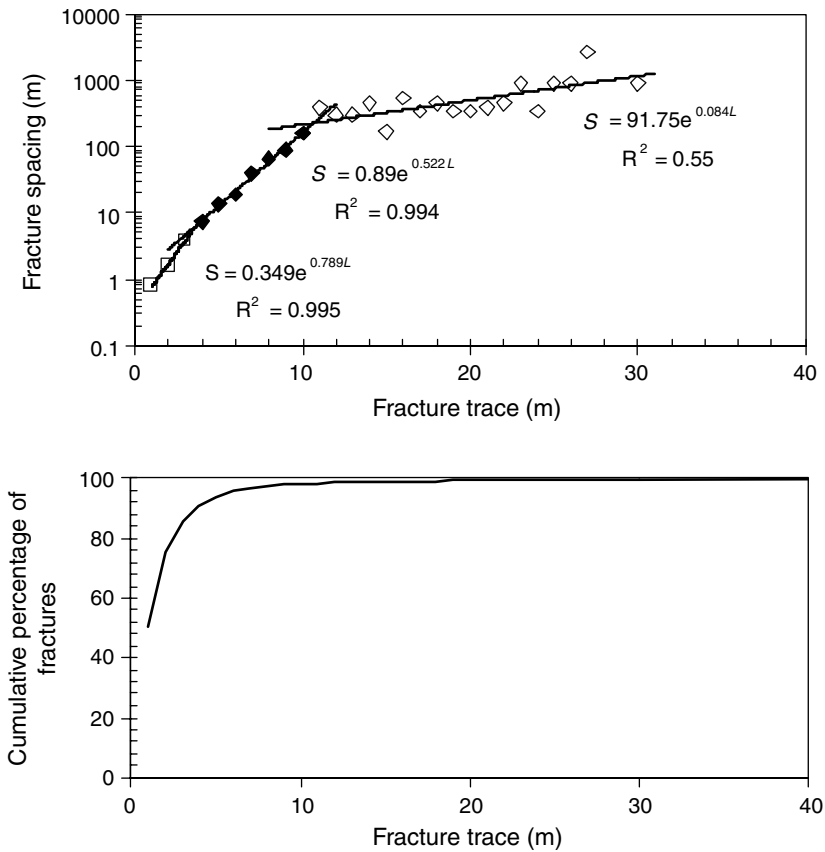


**FIGURE 20.13** Results from measurements of fracture characteristics for the TSw unit (nonlithophysal zone) along ESF between Stations 10+80 and 37+80: upper panel — relationship between the fracture spacing and the fracture trace length, showing three distinct segments that are assumed correspond to small, intermediate, and large scales; and lower panel — cumulative percentage of fractures vs. the fracture trace length.

spacing and fracture trace length. (The trace length was measured from the DLS [detailed line survey tape] to the discontinuity's upper end, and from the tape to its lower end, which exemplifies the persistence of discontinuities on the tunnel wall.) This figure shows three distinct segments of the relationship between fracture spacing and fracture trace length. Each segment is described by an exponential function given by:

$$S = \alpha \exp(\beta L) \quad (20.6)$$

where  $S$  is fracture spacing (in meters) and  $L$  is fracture trace length (in meters) along the tunnel. In the first segment (fracture length is up to 2 to 3 m), coefficients  $\alpha$  and  $\beta$  are 0.349 m and  $0.789 \text{ m}^{-1}$ ; in the second segment (the fracture length is between 2 and 10 m),  $\alpha$  and  $\beta$  are 0.89 m and  $0.522 \text{ m}^{-1}$ . In the third segment (the fracture length between 10 and 30 m),  $\alpha$  and  $\beta$  are 91.75 m and  $0.084 \text{ m}^{-1}$ .

We suggest that these segments correspond to small-, intermediate-, and large-scale hierarchical components of fractured tuff. The trace length of 2 m represents a critical fracture length separating small and intermediate scales. The length of 10 m represents a critical fracture length separating intermediate and large scales. Figure 20.13b shows that the number of small fractures of less than 1 m in length is about 50% of the total number of fractures, and the number of fractures up to 2 m is about 75% of the total number of fractures. Despite the fact that small-scale fractures (constituting a significant portion of the total fractures), may play a key role in flow and transport phenomena on the field scale, they are not implicitly represented in the large-scale Yucca Mountain numerical model with a gridblock size as much as 100 m.<sup>152</sup> Using the idea of hierarchy of scales, a summary of the types of fractures encountered at Yucca Mountain and the types of tests and measurements conducted at these scales is shown in Table 20.2.

## 2. Relationship between Hierarchical Components for Fractured Tuff

To present a relationship between hierarchical components for fractured tuff, Table 20.3 shows the main lithological and hydrogeological features at Yucca Mountain on different scales. If Level 0 investigations are conducted to develop a *large-scale* model of Yucca Mountain, including the study of flow and transport processes in different geologic layers with various dominant components, then Level -1 investigations include the processes in different geologic layers. The upper panel of Figure 20.12 illustrates the types of flow processes to be studied on Level -1: (1) lateral flow at the interface between TCw and PTn units, and dispersion in the PTn unit, and (2) the creation of a perched-water zone at the TSw-CHn interface, including dominant fracture flow in the TSw unit, dominant matrix flow in the vitric CHn unit, and diversion around the zeolitic CHn.

The lower panel of Figure 20.12 shows examples of: (1) flow convergence of a small-fracture network in the finely fractured zone of the Tptpul unit with a coarsely fractured zone in the Tptpmn unit, and (2) flow diversion from a coarsely fractured zone in the Tptpmn unit into the finely fractured zone in the Tptpll unit. Level +1 investigations involve ambient processes representing system boundary conditions, such as atmospheric processes (e.g., climate, temperature, barometric pressure, and groundwater table fluctuations). The large-scale barometric pressure fluctuations at the land surface affect changes in pneumatic pressure in the unsaturated subsurface.<sup>153,154</sup> The relationship between the surface barometric pressure fluctuations and the subsurface pressure response depends on the bulk pneumatic diffusivity of the rock layers, which, in turn, depends on the distribution and connectivity of fractures and faults.

If Level 0 investigations are conducted to develop an *intermediate-scale* model (for example, flow and transport processes in a fracture network around the tunnel), then Level -1 investigations include the study of field small-scale processes taking place in small fractures and lithophysal zones (including damp fractures, seepage, evaporation due to tunnel ventilation, intrafracture fingering). These processes may reduce the area of the fracture-matrix interaction. Inverse modeling confirmed

**TABLE 20.2**  
**Types of Fractures Encountered at Different Scales at Yucca Mountain and Types of Characterization Tests and Methods**

Hierarchical scale	Type of fractures and scales	Types of tests and measurements
Elemental scale	Microfractures (from millimeters to less than 20 to 30 cm in cores and to 1 m in rock blocks)	Laboratory cores (20 to 30 cm) and blocks (up to 1 m); monitoring probes are a few millimeters to several centimeters
Small scale	Small fractures (from centimeters to 2 to 3 m)	Minimum size corresponds to the size of miniature monitoring probes (e.g., tensiometer); the maximum size corresponds to the size of an infiltration pond (or a borehole air injection interval), and is limited by a critical length of a small-scale fracture Examples: infiltration and air-injection tests in niches at the cross drift of the enhanced characterization of the repository block (ECRB).
Intermediate scale	Intermediate fractures/shears (from less than 1 to 10 m)	Minimum size corresponds to the size of miniature monitoring probes (e.g., tensiometer); maximum size corresponds to the size of an infiltration pond and is limited by a critical scale of a fracture (10 m) Seepage studies in niches, Alcove 8/Niche 3, Alcove 1, air-injection tests (surface holes and alcoves)
Large scale	Large fractures/faults (from less than 10 m to 100s of meters)	Minimum size corresponds to the size of monitoring probes or testing intervals in boreholes. The maximum size is the length of faults extending over the distance of as much as 100s of meters.

**TABLE 20.3**  
**Summary of Main Lithological and Hydrogeological Features to be Considered Depending on the Scale of Investigations**

Scale		CLIMATE, INFILTRATION, TEMPERATURE, BAROMETRIC PRESSURE, WATER TABLE RISE/FALL										
Large	Intermediate	Tiva Canyon Tuff (TCw)			Yucca Mountain Tuff, Pah Canyon Tuff, and bedded tuffs (PTn)			Topopah Spring Tuff (TSw)			Calico Hills Formation (CHn)	
Level 1	Level 2	Welded xl-rich and xl-poor members			Nonwelded tuffs			Welded xl-rich and xl-poor members			Nonwelded tuffs	
Level 0	Level 1	Fracture networks			Matrix			Fracture networks			Matrix	
Level -1	Level 0	nonlithophysal zone	lithophysal zone	vitric zone	Yucca Mountain Tuff (Tpy)	Pah Canyon Tuff (Tpp)	bedded tuffs	nonlithophysal zone	lithophysal zone	vitric zone	vitric	zeolitic
Geologic layers		Dominant vertical flow in medium to large fractures			Flow dispersion in networks of small fractures; Role of litho cavities (cap. barriers)?			Dominant vertical flow in fractures			Flow dispersion in porous matrix; lateral flow above zeolites	
Dominant component		Flow dispersion in matrix where nonwelded			Flow dispersion in matrix where nonwelded			Flow dispersion in matrix; lateral flow caused by anisotropy and mineral ait.			Perched water; Mineral ait w/in fractures; Dominant vertical flow in fractures where unaltered	
Lithologic unit		Flow and transport processes			Flow and transport processes			Flow and transport processes			Flow and transport processes	
Flow and transport processes		Types of testing to study local flow and transport processes			Niche Studies			Alcove 6 - Fracture/Matrix test			Infiltration Experiments (0.3 m scale)	
		permeability estimated from borehole air-injection tests (0.3 m scale)			Seepage testing			Liquid dye experiments investigating flowpaths and F/M interaction			permeability estimated from borehole air-injection tests (0.3 m scale)	
								F/M interaction			Water balance studies	
								unsaturated permeability estimated			F/M interaction	

**TABLE 20.4**  
**Types of Models for Different Scales**

Models	Scales			
	Elemental	Small	Intermediate	Large
<b>Mechanistic</b>				
Macroscale continuum			+	+
High-resolution finite difference	+	+	+	
<b>Phenomenological</b>				
Transfer function	+	+	+	
Weeps				
Fractal	+	+	+	
Chaos	+	+		
<b>Network and percolation models</b>				
Fracture network		+	+	+
Percolation models	+	+	+	

*Note:* References to the models are given in the text.

that the fracture–matrix interface area (i.e., the area covered by flowing water) is approximately 1 to 3% of the fracture surface.<sup>155</sup> Figure 20.12(b,c) illustrates two types of flow processes: (1) lateral flow at the interface between TCw and PTn units as well as dispersion in the PTn unit, and (2) the creation of a perched-water zone at the TSw-CHn interface, including dominant fracture flow in the TSw unit, dominant matrix flow in the vitric CHn unit, and diversion around zeolitic CHn. Level +1 investigations used to assign boundary conditions for the intermediate-scale model should include the study of the whole TSw unit.

Level 0 field investigations conducted to study *small-scale* flow and transport processes are characterized as follows. Using air-injection tests at the proposed repository horizon, one can study fracture connectivity and heterogeneity. Seepage tests in niches can be used to determine the fracture–matrix interaction, such as Alcove 6 and Alcove 4 infiltration tests.<sup>156–158</sup> Level –1 investigations may involve elemental-scale investigations using laboratory single cores or field single probes. Examples of laboratory fracture experiments include film flow<sup>66</sup> and intermittent flow investigation through various fracture replicas.<sup>159</sup> Level +1 boundary conditions are assigned according to the intermediate- or large-scale investigations.

### 3. Infiltration and Air-Injection Tests on a Hierarchy of Scales

#### a. *Small-Scale Test*

Infiltration tests were carried out at two sites (Alcove 4 and Alcove 6) at Yucca Mountain's ESF. Alcove 4 tests investigated unsaturated flow processes within the Paintbrush nonwelded unit (PTn),<sup>156,158</sup> and Alcove 6 investigations were conducted in the middle nonlithophysal portion of the Topopah Spring welded tuff unit (TSw)<sup>157,158,160</sup> The analysis of infiltration rates measured at both sites showed three temporal scales of infiltration rate: (1) a *macroscale* trend of overall decreasing flow, (2) a *mesoscale* trend of fast and slow motion, exhibiting three-stage variations of the flow rate (decreasing, increasing, and again decreasing flow rate, as observed in soils in the presence of entrapped air), and (3) *microscale* (high-frequency) fluctuations.<sup>65</sup> Infiltration tests in the nonwelded unit at Alcove 4 indicate that this unit may effectively dampen episodic fast infiltration events. Infiltration tests in highly permeable, fractured, welded tuff at Alcove 6 indicate

that the infiltration rate exhibits pulsation possibly caused by multiple threshold effects or water–air redistribution between fractures and matrix, as well as between different fractures.

Infiltration tests showed that the wetting front in fractured rock progresses not only downward, but also is imbibed back into the matrix, increasing water travel time. Based on a comparison of temporal flow behavior in fractured rock (observed in a series of infiltration tests at Alcove 4) with that observed in porous media, Faybishenko et al.<sup>64</sup> suggested that the entrapped air is affecting hydraulic conductivity of tuffs and a one-dimensional Richards' equation (which assumes that the air phase cannot be “trapped”) is inadequate to describe infiltration in a fractured formation. This deficiency results from the equation's inability to account for gravity-driven flow with fingering effects in fractures,<sup>161</sup> as well as the redistribution of water and air between fractures and matrix. The detection of seepage from fractures in a series of field and laboratory infiltration tests indicates that fracture water is under positive pressure, while the matrix remains unsaturated and water in the matrix is under negative pressure. The coexistence of negative and positive water pressures on the local scale in unsaturated fractured rock indicates a different physics for the flow processes.

To capture the fact that some fractures are active (flow-through) while some are inactive (no-flow-through), Liu et al.<sup>162</sup> introduced an active-fracture model. In addition, to account for fracture flow dynamics and fracture–matrix interaction processes depending on temporal variations of the water content in fracture and matrix components of fractured rock, Faybishenko et al.<sup>64</sup> introduced a dynamic conceptual model of flow in fractured rock. When the infiltration rate increases in welded tuff, more fractures are likely to be involved in flow, thus intensifying the processes of extrinsic seepage, imbibition, and gravity drainage. As a result, seepage and imbibition rates are proportional to the infiltration rate, implying dynamic system behavior.

Figure 20.14 shows the dynamic fracture flow pattern and fracture-matrix imbibition in fractured rock, including (1) flow-through fractures, (2) dead-end fractures, (3) fractures connecting flow-through fractures, and (4) the matrix. This pattern implies that the increase in infiltration rate involves an additional flow in connecting and dead-end fractures, which also enlarges the area of the fracture-matrix interaction and increases matrix imbibition. Figure 20.14 also illustrates that water pressure,  $\Phi$ , which is measured in a certain volume of the formation, depends on the flow regime, i.e., it varies for different flow rates  $q_1$ ,  $q_2$ , and  $q_3$  and can be expressed as a function of moisture content  $\Theta$  and its time derivative  $d\Theta/dt$ . This conceptual model is consistent with the active fracture model of Liu et al.,<sup>162</sup> who hypothesized that only a saturation-dependent portion of connected fractures is active in conducting water. The Alcove 6 tests also showed high-frequency fluctuations in the infiltration and seepage rates within the middle nonlithophysal portion of the Topopah Spring welded tuff, which

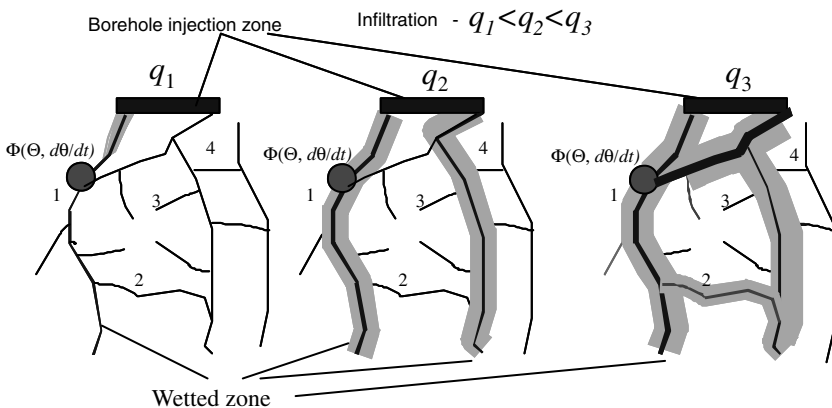


**FIGURE 20.14** Schematic of the dynamic fracture flow pattern and fracture matrix imbibition in fractured rock, including (1) flow-through fractures, (2) fractures connecting flow-through fractures, (3) dead-end fractures, and (4) the matrix. (From Faybishenko, B., Bodvarsson, G.S., and Salve, R., *J. Contam. Hydrol.*, in press, 2003)

are the main feature of nonlinear dynamic processes. That microscale fluctuations are chaotic is important, because such behavior is likely to generate chaotic and fractal chemical-diffusion processes in fractured tuff and thus affect the description of diffusion-reaction systems.

A series of small-scale infiltration tests at Alcove 6 showed that the travel time for the wetting front's leading edge is described by a power-law equation given by

$$T = \alpha q^\beta \tag{20.7}$$

where  $T$  is the water travel time,  $q$  is the infiltration rate, and  $\alpha$  and  $\beta$  are coefficients. Equation 20.7 implies scaling and self-similarity phenomena<sup>163</sup> for the waterfront geometry on the scale of measurement.

Because of local heterogeneity, the results of small-scale niche seepage studies are site specific, and not necessarily representative of seepage at other locations (even within the same geologic unit).

*b. Intermediate-Scale Infiltration Tests*

Intermediate-scale investigations around the tunnel, if conducted at Level 0, would involve several types of small-scale flow processes with measurements on Level -1, which are shown in Figure 20.15. To illustrate the intermediate-scale investigations, we will use the results of the ESF and Busted Butte infiltration tests.

*ESF Tests.* Infiltration experiments at Alcove 1 (located in the Tiva Canyon welded tuffs near the north portal of the ESF, closer to the land surface than the other test facilities) simulated flow that might occur as a result of high rainfall under future (wetter and cooler than present)

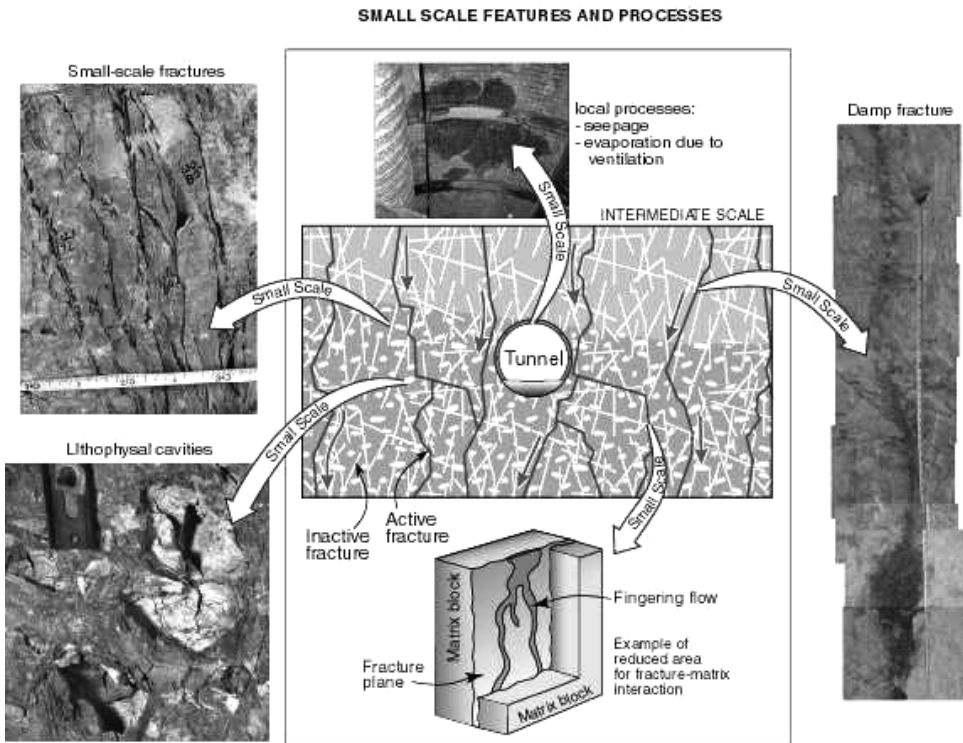


**FIGURE 20.15** (See color insert following page 144.) Illustration that the intermediate-scale investigations around the tunnel at Level 0 involve several types of small-scale flow processes (Level -1). Data from Wang, J.S. et al., ANL-NBS-HS-000005, Rev. 01, 2001, and Hinds, J.J. and Bodvarsson, G.S., presentation given at the 2001 International High-Level Radioactive Waste Management Conference.

climate conditions.<sup>8,158</sup> At the surface above the alcove, water was applied to a 91 m<sup>2</sup> area, while seepage at the roof of the alcove was observed within a 44.2 m<sup>2</sup> collection area, separated into plots of about 0.1 m<sup>2</sup> to detect the spatial distribution of the seepage rate. The initial water travel time from the surface to the collection system was 58 days (which could be caused by water imbibition into the initially unsaturated matrix), but after flow through a fracture system had been established, the changes in surface-water supply rate generated much faster corresponding changes in the seepage rate into the alcove — within a few days. This accelerated seepage rate into the alcove confirmed a relatively high hydraulic connectivity for water flow through the fracture network.

*Busted Butte.* The Unsaturated Zone Transport Test (UZTT) was conducted at Busted Butte of the Nevada Test Site (NTS), Nevada, 8 km southeast of the proposed repository area.<sup>164</sup> The site was chosen because it featured readily accessible exposure of unsaturated rocks from the Topopah Spring/Calico Hills formations, which are stratigraphic units beneath the potential repository. The test was designed to evaluate the effect of heterogeneities on flow and transport under unsaturated conditions in the Calico Hills, the effect of fracture–matrix interactions and permeability, and the migration behavior of colloids in fractured and unfractured Calico Hills rock. During the test, conservative and reactive tracers and polystyrene microspheres were injected through six injection wells, with collection in two boreholes, each 2 m in length and located in the Calico Hills formation and the Topopah Spring unit.

After 6 to 8 months of continuous injection, it was determined that the Calico Hills layer would present a physical and chemical barrier to radionuclide migration over a wide range of infiltration rates (30 to 400 mm/year) because of a strong retardation by the vitric matrix containing clay particles ( $4 \pm 2\%$ ). Strong retardation of chemicals observed under field conditions can be explained by large sorption coefficients determined from laboratory experiments in the vitric Calico Hills rocks. The Busted Butte test demonstrates that the vadose zone can act as a barrier to contaminant transport or as a fast pathway, depending on the boundary condition (infiltration rate) and on the Calico Hills hydraulic properties.

### c. Large-Scale Investigations

Large-scale hydrogeological properties can be characterized using the results of gas-flow injection tests or measurements of ambient barometric pressure fluctuations (above the land surface) or changes in pneumatic pressure measured at different depths in the subsurface.<sup>153,165</sup> The subsurface-pressure response to surface barometric changes is dominated by the bulk pneumatic diffusivity of rock as controlled by the distribution and connectivity of rock discontinuities (fractures and faults). A diffusive process of gas flow in a well-connected fracture system is likely to provide considerable intrarock averaging, which is amenable to modeling large-scale volume-averaged flow processes.<sup>153</sup>

### d. Variations of Permeability on Different Scales

The range of rock permeability characterizes volume averaging of hydraulic properties on different scales with much larger range of variations of hydraulic properties at smaller scale.<sup>99,166</sup> As the scale of field experiments increases, the average value of rock permeability (determined from air-injection tests conducted in boreholes) increases (see Figure 20.3, upper panel), whereas the magnitude of rock permeability variations decreases. At a 1-m scale, air permeability varies over five orders of magnitude, with an average value of approximately  $10^{-13}$  m<sup>2</sup>. On the scale of 1 to 10 m, air permeability spans about three orders of magnitude, with an average value between  $10^{-13}$  and  $10^{-12}$  m<sup>2</sup>. On the scale of 100 m, air-permeability values span about one order of magnitude, with an average value of  $\sim 10^{-11}$  m<sup>2</sup>. On a scale of 1000 m (including faults), air permeability spans less than one order of magnitude, between  $10^{-9}$  and  $10^{-10}$  m<sup>2</sup>. For each scale, small values of permeability can be indicative of matrix permeability (or the involvement of low-permeability dead-end fractures), with large values indicative of fracture permeability.

## V. MODELS OF FLOW PROCESSES ON A HIERARCHY OF SCALES

### A. TYPES OF MODELS

Many approaches have been used for mathematical modeling of flow and transport in unsaturated fractured rock, ranging from mechanistic cause-and-effect type models to empirical correlations with no detailed representation of physical processes.<sup>167</sup> However, Pruess et al.<sup>41</sup> concluded that no single approach could characterize completely and reliably a complex subsurface system. They recommended the use of two or more alternative modeling approaches simultaneously because different approaches may simulate different flow processes, based on the results of different types of measurements and the different physics involved in various models. Selection of a particular modeling approach or combination of approaches needs to be related to the practical objective of the study and the scale of investigations. Table 20.4 provides a summary of model types for different scales.

Detailed mechanistic process models could conceivably be substantiated using the results of observations and field experiments at the local scale, and can be used to represent much more spatial detail than those using volume-averaged models. Mechanistic models may also provide a conceptual model for verification of macroscale approaches.

Phenomenological models, such as weeps-type,<sup>168</sup> transfer function,<sup>169</sup> and chaos models,<sup>65</sup> can be used to complement detailed process models, such as high-resolution continuum models. Phenomenological models are simpler and require only a small set of parameters, and they are useful because of their conceptual simplicity, transparency, and robustness. They also require a minimum of assumptions and parameters whose validity, however, may be difficult to establish.<sup>41</sup> Chaos models are applicable to certain aspects of fluid flow and mass transport through fractured rock.<sup>65</sup> At Yucca Mountain, time-series records of environmental isotopes may be analyzed to reconstruct past infiltration history as affected by paleoclimatic change. Neutron-logging data and temperature, pressure, and water-level measurements should also be examined for chaotic processes. Evaluation of nuclear waste disposal capabilities or remediation technologies at different sites requires concurrent use of “complementary” aspects of different modeling approaches from different models, thereby reducing uncertainties in measurements and modeling.

### B. EXAMPLES OF MODELS

#### 1. Elemental Scale

Taking into account that elemental-scale flow experiments using fracture models showed the pulsating character of temporal pressure changes (under constant boundary conditions) in response to water and air injection (e.g., Persoff and Pruess<sup>62</sup>), Faybishenko<sup>65</sup> showed that pressure fluctuations could be described using a fourth-order partial differential equation known as the Kuramoto-Sivashinsky (K-S) equation:<sup>170,171</sup>

$$\frac{\partial \phi}{\partial \tau} + \phi \frac{\partial \phi}{\partial x} + \frac{\partial^2 \phi}{\partial x^2} + \frac{\partial^4 \phi}{\partial x^4} = 0 \quad (20.8)$$

where  $\phi$ ,  $x$  and  $\tau$  are dimensionless film thickness, length, and time, respectively. In the K-S equation, the second term is a nonlinear term, whereas the third and fourth are destabilizing and stabilizing terms, respectively, of the same order of magnitude, that describe dissipative processes.<sup>170,171</sup> The amplitude of fluctuations on average remains constant, but the attractor may display local fluctuations, with no systematic changes over time. (Note an *attractor* is a bounded region of the phase space to which all sufficiently close trajectories of the state vectors evolve in time from initial conditions.<sup>172</sup>) For the flow process in a fracture described by the K-S equation, we can reasonably

hypothesize that the linear relationship between the pressure head and the flow rate (i.e., Darcy's law) is invalid on a local scale, at least for the periods of chaotic fluctuations. Note that one of the criteria for chaos is that the flow process is not described by Darcy's law.<sup>173</sup> Equation 20.8, written in a canonical form, implies the possibility of scaling to determine characteristic time and length scale for dimensionless parameters used in this equation.

In a series of laboratory experiments in partially saturated fracture models, Geller et al.<sup>52</sup> illustrated the presence of intrafracture water-dripping phenomena, which were found to be chaotic.<sup>65</sup> Moreover, pressure data can be used to investigate dripping water frequency.<sup>52</sup> Results showed that low-dimensional chaotic attractors for water pressure developed in fracture replicas as a result of intrafracture water dripping.<sup>52,65</sup>

Assuming the locally valid cubic law for flow between slightly nonparallel plates, Nicholl and Detwiler<sup>174</sup> show that Reynolds' equation may overestimate steady incompressible flow by as much as 100% because of an inadequate description of head loss in the aperture-varying fracture. Nicholl and Detwiler introduced an ad hoc correction of Reynolds' equation, using an improved estimate of longitudinal dispersivity. Feder and Jossang<sup>30</sup> showed that, in a porous medium, the averaged solute transport behavior is accurately described by the convection-diffusion equation; however, on a small scale, the dispersion front, which has a fractal structure, depends on combined diffusion and random convection in the porous medium.

## 2. Small Scale

Several types of models can be used to describe small-scale water flow processes. Water dripping at a fracture exit (observed in 1-m scale HHA infiltration tests in fractured basalt<sup>63</sup>) is unstable and irregular in space and time, even under a constant ponded-water level. Time intervals between dripping-water events can be described by Equation 20.8.

Simulations using mechanistic process models to describe unsaturated media are commonly based on the application of Richards' equation

$$\frac{\partial \Theta(P)}{\partial P} \frac{\partial H}{\partial t} = \text{div} [K(P) \text{grad} H] + J \quad (20.9)$$

where  $t$  is time,  $\Theta$  is volumetric moisture content,  $K(P)$  is the unsaturated hydraulic conductivity function, and  $H$  is hydraulic head,  $H = P/\rho\gamma + z$ ,  $P$  is water pressure,  $\rho$  and  $\gamma$  are water density and gravity acceleration, respectively,  $z$  is a vertical coordinate and  $J$  is the source/sink that can be used to characterize the fracture-matrix interaction.

However, the parameters of Richards' equation, such as water-retention [ $\Theta(P)$ ] and unsaturated hydraulic conductivity [ $K(P)$ ] functions, may not even be meaningful for large-size discontinuous fractured rock because of the discontinuity condition for a flux at the fracture-matrix interface. (The conventional approach to determining these parameters involves inverse modeling techniques.) In this case, a continuous description of liquid motion by the differential equation becomes inadequate.<sup>175</sup> A discontinuity condition at the fracture-matrix interface arises from the effects of adsorbed liquid films at the fracture surface and the phase change. These films, which are regarded as insoluble in liquid, generate additional forces at the liquid free surface.<sup>176</sup> The phase change, which is affected by heat-mass transfer, requires consideration of a mass-balance equation, with an additional term describing an increase in mass at a phase-interface surface.<sup>119</sup>

If one intends to use Richards' equation to describe the infiltration rate at a small scale, an explicit presentation of a fracture pattern and fracture-matrix interaction is required. Since fast and slow types of flow occur during infiltration tests, we can infer that flow behavior can be described by a dual-continuum model of double-porosity or double-permeability media, with flow-rate-dependent functions for unsaturated hydraulic conductivity and water retention.

The fact that Philip's equation cannot satisfactorily describe the observed initial decrease in the infiltration rate suggests that flow processes other than those described by Richards' equation are involved in fractured-rock infiltration.<sup>64</sup> The dynamic effects of fracture–matrix interaction under infiltration can be introduced into the flow model by using a time-dependent (or flow-rate-dependent) moisture content, which will characterize the redistribution of water between the fracture and the matrix (see Figure 20.14). For example, the water pressure  $P$  can be expressed as a function of the moisture content  $\Theta$  and its time derivative,  $d\Theta/dt$ :

$$P = f(\Theta, d\Theta/dt) \quad (20.10)$$

The application of this concept will lead to Hallaire's model<sup>177</sup> for flow in partially saturated media, developed for structured soils (which was further applied to water flow and evaporation by Rode<sup>178</sup> and Feldman<sup>179</sup>).

$$\begin{aligned} \frac{\partial \Theta}{\partial t} &= \frac{d}{dx} \left( D \frac{\partial \Theta}{\partial x} + A \frac{\partial^2 \Theta}{\partial x \partial t} \right) \\ D &= k \frac{\partial P}{\partial \Theta} \\ A &= k \frac{\partial P}{\partial \left( \frac{\partial \Theta}{\partial t} \right)} \end{aligned} \quad (20.11)$$

### 3. Intermediate Scale

Depending on the type of fracturing, a random or deterministic (explicit) presentation of the geometry of a fracture network can be used for modeling. For example, two-dimensional numerical modeling of the Box Canyon ponded-infiltration tests based on Richards' equation (using the TOUGH2 code), with a random presentation of fractures, did not match the results of the infiltration test, whereas the deterministic presentation of a fracture system provided a good match.<sup>139</sup> Modeling results suggest that despite the fact of a deterministic presentation of the fracture system, coupled effects of flow funneling, the decrease in the rock permeability with depth, and air entrapment and escaping contribute to the decrease in infiltration rate. This type of modeling, however, could not capture the temporal aspects of chaotic flow identified in laboratory and small-scale field experiments.

According to Doughty,<sup>180</sup> who investigated various conceptual and numerical approaches for modeling flow and transport processes in the unsaturated zone at Yucca Mountain, a one-dimensional modeling of steady-state moisture flow, using various models, provides similar results for saturation and fracture flow profiles. The equivalent continuum media (ECM) approach can be used to model the steady-state processes adequately, given the near-equilibrium condition for the fracture–matrix interaction. However, transient moisture flow and transport cannot be simulated using the ECM. Within dual-continuum models, the effect of fracture–matrix interface can significantly affect an infiltration pulse and tracer arrival at various depths. The results of modeling depend also on the space discretization used in the numerical model. For example, the increase in a number of matrix gridblocks yields slower fracture response times. For transient gas flow in the subsurface caused by barometric pressure fluctuations, the ECM adequately models the process because the time scale of subsurface pressure fluctuations is comparable to that of the barometric pressure fluctuations. However, the ECM may not capture all the physical processes involved in thermal transport because of relatively rapid fluid flow and heat transport in fractures, which are not in equilibrium with the matrix.

#### 4. Large Scale

Macroscale continuum modeling of unsaturated zone flow and transport at Yucca Mountain employs large-scale volume averaging to homogenize heterogeneous fracture and matrix permeabilities, and to average spatially variable infiltration rates applied at the land surface.<sup>181,182</sup> Volume-averaged concepts typically predict downward water migration proceeding in the form of smooth sheets, accompanied by imbibition into the partially saturated rock matrix.<sup>183–186</sup> For an average net infiltration on the order of 5 mm/year, the water velocity in fractures at Yucca Mountain (based on the active fracture model by Liu et al.<sup>162</sup>) is on the order of several meters per year in the welded units, and the calculated velocity can be as high as 50 m/year, depending on model parameters. For comparison, a piston-style percolation of water would require thousands of years to reach the water table at Yucca Mountain.<sup>41</sup>

Large-scale three-dimensional process models of the unsaturated zone at Yucca Mountain include models of moisture and gas flow processes,<sup>152,153,181,187</sup> radionuclide transport,<sup>182,188</sup> and mountain-scale thermohydrology.<sup>189</sup> Flow models have been constrained by field measurements of water saturations and moisture tensions measured in boreholes,<sup>155</sup> pneumatic data from instrumented boreholes,<sup>153</sup> geochemical isotope and mineral data,<sup>190,191</sup> perched-water data,<sup>152</sup> and temperature data.<sup>155</sup> However, several different conceptual models may be consistent with the bulk of the available information, implying a nonuniqueness of predictions.<sup>41</sup> Most of the above models use the dual-permeability formulation, including fracture and matrix continua flow and transport.

A promising approach to modeling large-scale phenomena uses a system of ordinary, time-delayed differential equations to simulate the chaotic dynamics of moisture content and infiltration rate in a hydraulically active zone, for annual and seasonal variations of precipitation. Such a model was used by Rodriguez-Iturbe et al.<sup>192,193</sup> for precipitation and soil moisture predictions. Another alternative is the use of a three-dimensional, fine- or coarse-resolution model, taking into account fracture-network geometry and the fracture–matrix interaction.<sup>41</sup>

## VI. DISCUSSION AND CONCLUSIONS

A key question that faces soil scientists and hydrogeologists is whether flow processes in unsaturated fractured rock can be analyzed using the same measurements and models regardless of scale. To answer this question, we first illustrated the causes of a complex, spatial–temporal behavior of unsaturated flow and transport in fractured rocks, and then demonstrated the difference between the concepts of scaling and a hierarchy of scales to be used to describe a complex, spatial–temporal behavior of unsaturated flow and transport in fractured rocks.

Field and modeling investigations in unsaturated, discontinuous, fractured systems encompass a considerable range of spatial (i.e., rock-matrix pore structure, microfractures, fracture networks) and temporal scales over the field site. Examples of such processes of water flow are: preferential and fast flow, funneling and divergence of flow paths, transient flow behavior, nonlinearity, unstable and chaotic flow regimes, and fracture–matrix interaction phenomena.

Knowledge about the physics of flow processes and an understanding of the geometry of a fracture network are essential for predicting flow and transport over large scales under field conditions. However, point-type measurements using single probes in a fractured rock cannot reveal complex (mostly, nonlinear) processes that result from the interaction of flow processes in fractures and matrix occurring at many different scales. The value of measuring flow parameters through a single fracture, using rock cores or fracture models under laboratory conditions, is practically the same as measuring parameters of flow through a single pore in porous media in order to predict the hydraulic properties of soils on a field scale. The behavior of preferential flow in a single fracture cannot explain the behavior of the rock system on a larger field scale because different physical processes are involved in flow processes on different scales.

Water flow in a fracture network embedded in a low-permeability matrix depends strongly on the interconnection of fractures. Because unsaturated flow processes are neither physically nor geometrically analogous to small-scale intrafracture flow processes or large-scale fracture-network processes, scaling techniques developed for porous media may not be appropriate for fractured rock. That different physical processes govern flow and transport processes on different scales, and that different mathematical models should describe these processes, is important for predictions of flow and transport in fractured rock.

Field and laboratory observations carried out on different scales capture only patterns and processes relevant to the scales and types of observations. Consequently, the conventional approach of collecting as much field and laboratory data as possible, and then volume averaging these data, may not be valid for unsaturated fractured rock. This is mainly because of the nonlinearity and the discontinuous flow and transport processes in discrete segments of fractured-porous media.

Models for flow through heterogeneous media were mostly developed without considering the possible inconsistency between the physics of small-scale measurements and the physics of processes incorporated in numerical models at different scales. The conventional approach to spatial and temporal averaging of flow parameters may create errors in predictions of water seepage and chemical transport through unsaturated fractured rocks, and lead to the underestimation of water travel time and breakthrough of chemicals.<sup>41</sup> Traditional concepts of volume averaging and scaling for unsaturated flow parameters are difficult to apply to fractured rock because different nonlinear processes tend to dominate within different characteristic domains in fractured media. One of the alternative approaches to this problem of scale and scaling in fractured rock is based on the concept of a hierarchy of scales. The hierarchy approach represents a system structure or the classification of a graded (ranked) series of system parts (subsystems), with each subsystem dominant over those below it and dependent on those above it.

Based on an analysis of experimental laboratory and field data, we employed the following hierarchical scales for fractured basalt and fractured tuff:

1. *Elemental scale* — laboratory cores or a single fracture at a field site
2. *Small scale* (approximately 0.1 to 1 m<sup>2</sup>) — representing flow and mass transport in a single fracture, including the fracture–matrix interaction, film flow and dripping water phenomena
3. *Intermediate scale* (approximately 10 to 100 m<sup>2</sup>) — representing flow in the fracture network on a field scale
4. *Large (regional) scale* — representing the fracture and fault network geometry

Measurements on a hierarchy of scales may require skipping some scales so that only the scales of measurement are considered. In the case of a hierarchy of scales, in order to extrapolate the results of a small-scale model to a large-scale model, we must find the expected value of the small-scale processes distributed across the larger scale. The remaining question is how data obtained on the small scale (by carrying out laboratory or small-scale field tests) can be used to understand large-scale field phenomena.

Models of flow and transport for different spatial and temporal levels of a hierarchy of scales must theoretically be independent of each other because different physical variables govern flow processes on different spatial scales. Thus, models are intended to simulate different physical processes on different scales. In practice, however, limitations exist in the field instrumentation used for measurements in fractured rock at different hierarchical scales. As a consequence the results of measurements and predictions appear to be dependent on scale.

The main difference between scaling and using a hierarchy of scales is that the scaling approach is based on using the same model with scaled parameters, whereas the hierarchy of scales is based

on using different models for each of the hierarchical levels. However, the scale of direct measurements remains the same for all types of conventional field experiments in the vadose zone (except for flow rate), so increasing the scale of an experiment allows the investigator to obtain more measurements; the physical meaning of each measurement remains the same regardless of the experiment. Using the same models for simulating flow and transport processes taking place at different scales, and field monitoring providing volume-averaged measurements, may be inconsistent with the real physical processes occurring at different scales and cause the uncertainty in predictions of flow and transport in unsaturated fractured rock.

## VII. ACKNOWLEDGMENTS

Reviews by André Unger, H.H. Liu, and Daniel Hawkes are very much appreciated. This work was partially supported by the Director, Office of Civilian Radioactive Waste Management, U.S. Department of Energy, and by the Director, Office of Science, Office of Basic Energy Sciences, the Environmental Management Science Program of the U.S. Department of Energy under Contract No. DE-AC03-76SF00098.

## REFERENCES

1. Mayer, S., Ellsworth, T.R., Corwin, D.L. and Loague, K., Identifying effective parameters for solute transport models in heterogeneous environments, in: *Assessment of Non-Point Source Pollution in the Vadose Zone*, D.L. Corwin, K. Loague, and T.R. Ellsworth, Eds., AGU, Washington, D.C., 119, 1999.
2. Wu, J., Hierarchy and scaling: extrapolating information along a scaling ladder, *Can. J. Remote Sensing*, 25(4), 367, 1999.
3. Hillel, D. and Elrick, D.E. (Eds.), *Scaling in Soil Physics: Principles and Applications*, Proceedings of a Symposium, SSSA Special Publication No. 25, Madison, WI, 1990.
4. Kutílek, M. and Nielsen, D.R., *Soil Hydrology*, Cremlingen-Destedt, Germany: Catena Verlag, 1994.
5. Sposito, G. (Ed.), *Scale Dependence and Scale Invariance in Hydrology*, Cambridge University Press, New York, 1998.
6. Haverkamp, R., Parlange, J.-Y., Cuenca, R., Ross, P.J., and Steenhuis, T.S., Scaling of the Richards equation and its application to watershed modeling, in: *Scale Invariance and Scale Dependence in Hydrology*, Cambridge University Press, Sposito G., Ed., Cambridge, Chapter 7, 1998.
7. Bodvarsson, G.S., Liu, H.H., Ahler, F., Wu, Y.S., and Sonnenthal, E., Parameterization and upscaling in modeling flow and transport in the unsaturated zone of Yucca Mountain, in: *Conceptual Models of Flow and Transport in the Fractured Vadose Zone*, National Academy Press, 335, 2001.
8. Liu, H.H. and Bodvarsson, G.S., Constitutive relations for unsaturated flow in a fracture network, *J. Hydrol.*, 252, 116, 2001.
9. Liu, H.H., Haukwa, C.B., Ahlers, C.F., Bodvarsson, G.S., Flint, A.L., and Guertal, W.B., Modeling flow and transport in unsaturated fractured rock: an evaluation of the continuum approach, *J. Contaminant Hydrol.*, in press, 2003.
10. Evans, D.D. and Nicholson T.J. (Eds.), *Flow and Transport through Unsaturated Fractured Rock*, Geophysical Monograph Series 42, American Geophysical Union, Washington, D.C., 1987.
11. Bear, J., Tsang, C.F. and de Marsily, G., Eds., *Flow and Contaminant Transport in Fractured Rock*, Academic Press, San Diego, CA, 1993.
12. Lee, C.-H. and Farmer, I., *Fluid Flow in Discontinuous Rocks*, London; New York: Chapman & Hall, 1993.
13. National Research Council Committee on Fracture Characterization and Fluid Flow, *Rock Fractures and Fluid Flow: Contemporary Understanding and Applications*, National Academy Press, Washington, D.C., 1996.
14. Corwin, D.L., Loague, K., and Ellsworth, T.R., Eds., *Assessment of Non-Point Source Pollution in the Vadose Zone*, Washington, D.C., American Geophysical Union, Geophysical Monograph 108, 1999.

15. Faybishenko, B., Witherspoon, P.A., and Benson, S.M., Eds., *Dynamics of Fluids in Fractured Rock*, Geophysical Monograph No. 122, AGU, 2000.
16. Evans, D.D., Nicholson, T.J., and Rasmussen, T., Eds., *Flow and Transport through Unsaturated Fractured Rock*, Geophysical Monograph Series No. 42, 2nd Ed., AGU 2001.
17. Clauser, C., Permeability of crystalline rocks, *EOS Trans. Am. Geophys. Union*, 73, 233–237, 1992.
18. Gale, J.E., Fracture properties from laboratory and large scale field tests: evidence of scale effects, in: *Scale Effects in Rock Masses*, da Cunha, Ed., *Proc. 2nd Int. Workshop Scale Effects Rock Masses*, Lisbon, Portugal, June 25, 1993, pp. 341–352, 1993.
19. Koestler, A., Beyond atomism and holism — the concept of the holon. Beyond reductionism, new perspectives in the life sciences, in *Proc. Alpbach Symp.* [1968], Koestler, A. and Smythies, J.R., Eds., 192, Hutchinson, London, 1969.
20. Simon, H.A., *The Sciences of the Artificial*, MIT Press, Cambridge, MA, 1969.
21. Schultz, A.M., The ecosystem as a conceptual tool in the management of natural resources, in *Natural Resources: Quality and Quantity*, Cieriacy-Wantrup, S.V., Ed., 139, University of California Press, Berkeley, 1967.
22. Overton, W.S., Toward a general model structure for forest ecosystems, in *Proc. Symp. Res. Coniferous Forest Ecosyst.*, Franklin, J.F., Ed., Northwest Forest Range Station, Portland, Oregon, 1972.
23. MacMahon, J.A., Phillips, D.L., Robinson, J.V., and Schimpf, D.J., Levels of biological organization: an organism-centered approach, *Bioscience*, 28, 700, 1978.
24. Webster, J.R., Hierarchical organization of ecosystems, in *Theoretical Systems Ecology*, Halfon, E., Ed., 119, Academic Press, New York, 1979.
25. Allen, T.F.H. and Starr, T.B., *Hierarchy: Perspective for Ecological Complexity*, University of Chicago Press, Chicago, 1982.
26. O'Neill, R.V., De Angelis, D.L., Waide, J. B., and Allen, T.F.H., *A Hierarchical Concept of Ecosystems*, Princeton University Press, Princeton, New Jersey, 1986.
27. Ahl, V. and Allen, T.F.H., *Hierarchy Theory: a Vision, Vocabulary, and Epistemology*, New York, Columbia University Press, 1996.
28. Wu, J., Gao W., and Tueller, P.T., Effects of changing spatial scale on the results of statistical analysis with landscape data: a case study, *Geogr. Inf. Sci.*, 3, 30, 1997.
29. Wagenet, R.J. and Hutson, J.L., Scale-dependency of solute transport modeling/GIS applications, *J. Environ. Qual.*, 25(3), 499, 1996.
30. Feder, J. and Jossang, T., Fractal patterns in porous media, in *Fractals in Petroleum Geology and Earth Processes*, Barton, C.C. and La Pointe, P.R., Eds., Plenum Press, New York, 179, 1995.
31. Faybishenko, B.A., *Water-Salt Regime of Soils Under Irrigation*, Moscow, Agropromizdat. 314, 1986.
32. Faybishenko, B., Witherspoon, P.A., Doughty, C., Geller, J., Wood, T., and Podgorney, R., Multi-scale investigations of liquid flow in a fractured basalt vadose zone, in *Flow and Transport through Unsaturated Fractured Rock*, Geophysical Monograph No. 42, 2nd Ed., Evans, D.D., Nicholson, T.J., and Rasmussen, T., Eds., AGU, Washington, D.C., 161, 2001.
33. Weaver, W., Science and complexity, *Am. Sci.*, 36, 1948.
34. Wierenga, P.J., Hills, R.G., and Hudson, D.B., The Las Cruces trench site: experimental results and one dimensional flow predictions, *Water Resour. Res.*, 27, 2695, 1991.
35. Selker, J.S., Steenhuis, T.S., and Parlange, J.Y., Wetting-front instability in homogeneous sandy soils under continuous infiltration, *Soil Sci. Soc. Am. J.*, 56(5), 1346, 1992.
36. Sililo, O.T.N. and Tellam, J. H., Fingering in unsaturated zone flow: a qualitative review with laboratory experiments on heterogeneous systems, *Groundwater*, 38(6), 864, 2000.
37. Nativ, R., Adar E., Dahan, O., and Geyh, M., Water recharge and solute transport through the vadose zone of fractured chalk under desert conditions, *Water Resour. Res.*, 31, 2, 253, 1995.
38. Dahan, O., Nativ, R., Adar, E.M., Berkowitz, B., and Ronen, Z., Field observation of flow in a fracture intersecting unsaturated chalk, *Water Resour. Res.*, 35(11), 3315, 1999.
39. Weisbrod, N., Nativ, R., Ronen, D., and Adar, E., On the variability of fracture surfaces in unsaturated chalk, *Water Resour. Res.*, 34(8), 1881–1888, 1998.
40. Or, D. and Ghezzehei T.A., Dripping into subterranean cavities from unsaturated fractures under evaporative conditions, *Water Resour. Res.*, 36(2), 381–394, 2000.

41. Pruess, K., Faybishenko, B., and Bodvarsson, G.S., Alternative concepts and approaches for modeling flow and transport in thick unsaturated zones of fractured rocks, *J. Contaminant Hydrol.* Special Issue, 38, 281–322, 1999.
42. Birkholzer, J., Li G., Tsang C.-F., and Tsang, Y., Modeling studies and analysis of seepage into drifts at Yucca Mountain, *J. Contaminant Hydrol.*, 38(1–3), 349–384, 1999.
43. Lenormand, R. and Zarcone, C., Capillary fingering: percolation and fractal dimension, *Transport Porous Media*, 4, 599, 1989.
44. Glass, R.J., Modeling gravity-driven fingering in rough-walled fractures using modified percolation theory, in: *Proc. High Level Radioactive Waste Manage. Conf.*, Las Vegas, NV, American Nuclear Society, La Grange Park, IL., 2, 2042–2052, 1993.
45. Nicholl, M.J., Glass, R.J., and Nguyen, H.A., Wetting front instability in an initially wet unsaturated fracture, in *Proc., 4th High Level Radioactive Waste Manage. Int. Conf.*, Las Vegas, NV, Published by American Nuclear Society and American Society of Civil Engineers, 1993.
46. Glass, R.J., Parlange, J.-Y., and Steenhuis, T.S., Wetting front instability: 2. Experimental determination of relationship between system parameters and two-dimensional unstable flow field behavior in initially dry porous media, *Water Resour. Res.*, 25, 1195, 1989.
47. Glass, R.J., Rajaram, H., Nicholl, M.J., and Detwiler, R.L., The interaction of two fluid phases in fractured media, *Curr. Opinion Colloid Interface Sci.*, 6(3), 223, 2001.
48. Faybishenko, B.A., Hydraulic behavior of quasi-saturated soils in the presence of entrapped air: laboratory investigations, *Water Resour. Res.*, 31(10), 2421, 1995.
49. Faybishenko, B., Comparison of laboratory and field methods for determining quasi-saturated hydraulic conductivity of soils, in *Characterization and Measurement of the Hydraulic Properties of Unsaturated Porous Media*, Proc. Int. Workshop held in Riverside, California, October 22–24, 1997, M.Th. vanGenuchten, F.J. Leij, and L. Wu, Eds., 279, 1999.
50. Faybishenko, B., Doughty, C., Steiger, M., Long, J., Wood, T., Jacobsen, J., Lore, J., and Zawislanski, P., Conceptual model of the geometry and physics of water flow in a fractured basalt vadose zone, *Water Resour. Res.*, 37(12), 3499, 2000.
51. Su, G.W., Geller, J.T., Pruess, K., and Wen, F., Experimental studies of water seepage and intermittent flow in unsaturated, rough-walled fractures, *Water Resour. Res.*, 35(4), 1019, 1999.
52. Geller, J.T., Borglin, S., and Faybishenko, B., Water seepage in unsaturated fractures: experiments of dripping water in fracture models and chaos analysis, Report LBNL-48394, Lawrence Berkeley National Laboratory, Berkeley, CA, 2001.
53. Stothoff, S. and Or, D.A., Discrete-fracture boundary integral approach to simulating coupled energy and moisture transport in a fractured porous medium, in *Dynamics of Fluids in Fractured Rock*, Faybishenko, B., Witherspoon, P.A., and Benson, S.M., Eds., Geophysical Monograph 122, AGU, 267, 2000.
54. da Cunha, A.P., Ed., Scale effects in rock masses, *Proc. 2nd Int. Workshop Scale Effects in Rock Masses*, Lisbon, Portugal, 25 June 1993. Rotterdam; Brookfield: A.A. Balkema, 1993.
55. Brooks, R.H. and Corey, A.T., Hydraulic properties of porous media, *Hydrology Paper*, Vol.3. Colorado State University, Fort Collins, 1, 1964.
56. Gardner, W.R., Measurement of capillary conductivity and diffusivity with a tensiometer, *Trans. 7th Int. Congr. Soil Sci.*, Vol.1. Madison, WI, Elsevier, Amsterdam, 300, 1960.
57. van Genuchten, M. Th., A closed-form equation for predicting the hydraulic conductivity of unsaturated soils, *Soil Sci. Soc. Am. J.*, 44, 892, 1980.
58. Millington, R.J. and Quirk, J.M., Permeability of porous solids, *Trans. Faraday Soc.*, 57, 1200, 1961.
59. Acheson, D., *From Calculus to Chaos: an Introduction to Dynamics*, Oxford University Press, 1997.
60. Prazak, J., Sir, M., Kubik, F., Tywoniak, J., and Zarcone, C., Oscillation phenomena in gravity-driven drainage in coarse porous media, *Water Resour. Res.*, 28(7), 1849, 1992.
61. Fourar, M., Bories, S., Lenormand, R., and Persoff, P., Two-phase flow in smooth and rough fractures: measurement and correlation by porous-medium and pipe flow models, *Water Resour. Res.*, 29(11), 3699, 1993.
62. Persoff, P. and Pruess, K., Two-phase flow visualization and relative permeability measurement in natural rough-walled rock fractures, *Water Resour. Res.*, 31(5), 1175, 1995.

63. Podgorney, R., Wood, T., Faybishenko, B., and Stoops, T., Spatial and temporal instabilities in water flow through variably saturated fractured basalt on a one-meter scale, *Geophysical Monograph No. 122: Dynamics of Fluids in Fractured Rock*, Faybishenko, B., Witherspoon, P.A., and Benson, S.M., Eds., AGU, Washington, D.C., 129, 2000.
64. Faybishenko, B., Bodvarsson, G.S., and Salve, R., On the physics of unstable infiltration, seepage, and gravity drainage in partially saturated tuffs, *J. of Contam. Hydrol.*, in press, 2003.
65. Faybishenko, B., Chaotic dynamics in flow through unsaturated fractured media, *Adv. Water Resour.*, 25/7, 793, 2002.
66. Tokunaga, T.K., Wan, J., and Sutton, S.R., Transient film flow on rough fracture surfaces, *Water Resour. Res.*, 36(7), 1737, 2000.
67. Deriagin, B.V., Churaev, N.V., and Muller, V.M., *Poverkhnostnye Sily (Surface Forces)*, Nauka, Moskva, 1985.
68. Barker, J. A., A generalized radial flow model for hydraulic tests in fractured rock, *Water Resour. Res.*, 24(10), 1796, 1988.
69. Jourde, H., Pistre, S., Perrochet, P., and Drogue, C., Origin of fractional flow dimension to a partially penetrating well in stratified fractured reservoirs. New results based on the study of synthetic fracture networks, *Adv. Water Resour.*, 25, 371, 2002.
70. van Tonder, G., Riemann, G., and Dennis, I., Interpretation of single-well tracer tests using fractional-flow dimensions. Part 1: Theory and mathematical models, *Hydrogeol. J.*, 10, 351, 2002.
71. Riemann, K., van Tonder, G., and Dzanga, P., Interpretation of single-well tracer tests using fractional-flow dimensions. Part 2: A case study, *Hydrogeol. J.*, 10, 357, 2002.
72. Pachepsky, Ya., Benson, D., and Rawls, W., Simulating scale-dependent solute transport in soils with the fractional advective-dispersive equation, *Soil Sci. Soc. Am. J.*, 64(4), 1234, 2000.
73. Carr, J.R., Fractal characterization of and joint surface roughness in welded tuff at Yucca Mountain, Nevada, in *Proc. 30th U.S. Symp. Rock Mechanics*, Morgantown, WV, Khair, A.W., Ed., (Balema, Rotterdam), 193, 1989.
74. Long, J.C.S., Doughty, C., Hestir, K., and Martel, S., Modeling heterogeneous and fractured reservoirs with inverse methods based on iterated function systems, *Reservoir Characterization*, III, 471, Penwell Books, Tulsa, Oklahoma, 1991.
75. Perfect, E., Fractal models for the fragmentation of rocks and soils: a review. *Eng. Geol.*, 48(3-4), 185, 1997.
75. Crawford, J., Baveye, P., Grindrod, P., and Rappoldt, C., Application of fractals to soil properties, landscape patterns and solute transport in porous media, in Corwin, D.L., Loague, K., and Ellsworth, T.R., Eds., *Assessment of Non-Point Source Pollution in the Vadose Zone*, Geophysical Monograph 108, American Geophysical Union, Washington, D.C., 1999, 151.
76. Pachepsky, Ya. and Timlin, D.J., Water transport in soils as in fractal media, *J. Hydrol.*, 204, 98, 1998.
77. Dubois, J., *Non-linear Dynamics in Geophysics*, John Wiley & Sons, Chichester, U.K. (published in association with Praxis Pub.), 1998.
78. Turcotte, D.L., *Fractals and Chaos in Geology and Geophysics*, Cambridge, U.K.; New York: Cambridge University Press, 1997.
79. Unger, A.J., Bodvarsson, G.S., Faybishenko, B., and Simmons, A.M., Preferential flow paths in variably fractured basalt at the Box Canyon site, Idaho, *Lawrence Berkeley National Laboratory Report LBNL-44613*, 1999.
80. Janosi, I.M. and Horvath, V.K., Dynamics of water droplets on a window pane, *Phys. Rev. A*, 40(9), 5232, 1989.
81. Cushman, J.H., On measurement, scale, and scaling, *Water Resour. Res.*, 22(2), 129, 1986.
82. Faybishenko, B. and Finsterle, S., Tensiometry in fractured rocks, in *Theory, Modeling, and Field Investigation in Hydrogeology: A Special Volume in Honor of Shlomo P. Neuman's 60th Birthday*, Zhang, D. and Winter, C.L., Eds., Boulder, Colorado, Geological Society of America Special Paper 348, 161, 2000.
83. Hubbard, S., Rubin, Y., and Majer, E., Geophysical characterization of the vadose zone, in *Vadose Zone, Science and Technology Solutions*, Looney, B. and Falta, R., Eds., Batelle Press, 215, 2000.
84. Majer, E.L., Peterson, J.E., Daley, T., Kaelin, B., Myer, L., Queen, J., D'Onfro, P., and Rizer, W., Fracture detection using crosswell and single well surveys, *Geophysics*, 62(2), 495, 1997.

85. Neuman, S.P., Universal scaling of hydraulic conductivities and dispersivities in geologic media, *Water Resour. Res.*, 26(8), 1749, 1990.
86. Renshaw, C.E., Sample bias and the scaling of hydraulic conductivity in fractured rock, *Geophysical Res. Lett.*, 25 (1), 121, 1997.
87. Dagan, G., *Flow and Transport in Porous Formations*, Springer-Verlag Heidelberg Berlin New York, 1989.
88. Gelhar, L.W., *Stochastic Subsurface Hydrology*, Englewood Cliffs, NJ.: Prentice-Hall, 1993.
89. Neuman, S.P., Generalized scaling of permeabilities: validation and effect of support scale, *Geoph. Res. Lett.*, 21(5), 349, 1994.
90. Molz, F.J. and Boman, G.K., Further evidence of fractal structure in hydraulic conductivity distributions, *Water Resour. Res.*, 22(18), 2545, 1995
91. Hardy, H.H. and Beier, R.A., *Fractals in Reservoir Engineering*, World Scientific, Singapore, 1994.
92. Di Federico, V. and Neuman S.P., Scaling of random fields by means of truncated power variograms and associated spectra, *Water Resour. Res.*, 33(5), 1075, 1997.
93. Winter, C.L. and Tartakovsky, D.M., Theoretical foundation for conductivity scaling, *Geoph. Res. Lett.*, 2001.
94. West, G.B., Brown, J.H., and Enquist, B.J., A general model for the origin of allometric scaling laws in biology, *Science*, 276, 122, 1997.
95. Neuman, S.P. and Di Fredirico, V., Correlation, flow, and transport in multiscale permeability fields, in *Scale Dependence and Scale Invariance in Hydrology*, Sposito, G., Ed., Cambridge University Press, New York, 354, 1998.
96. Wheatcraft, S.W., J.H. Cushman Hierarchical Approaches to Transport in Heterogeneous Porous Media. *Revs. of Geophysics. Supplement - U.S. National Report to International Union of Geodesy and Geophysics 1987–1990*, 263, 1991.
97. Schultze-Makuch, D., Carlson, D.A., Cherkauer, D.S., and Malik, P., Scale dependency of hydraulic conductivity in heterogeneous media, *Groundwater*, 37(6), 904, 1999.
98. Sanchezvila, X., Carrera J., and Girardi, J.P., Scale effects in transmissivity, *J. Hydrol.*, 183(1–2), 1, 1996.
99. Nimmo, J.R., Meter-to-kilometer scaling of preferential flow in the unsaturated zone, in: Proc. Int. Sym. *Bridging the Gap between Measurements and Modeling in Heterogeneous Media*, 550, Berkeley, 2002.
100. Butler J.J. and Healey, J.M., Relationship between pumping-test and slug-test parameters — scale effect or artifact, *Ground Water*, 36(2), 305, 1998.
101. Tillotson P.M. and Nielsen, D.R., Scale factors in soil science, *Soil Sci. Soc. Am. J.* 48(5), 953, 1984.
102. Warrick, A.W., Application of scaling to the characterization of spatial variability in soils, in *Scaling in Soil Physics*, Hillel, D. and Elrick, D.E., Eds., Soil Science Society of America, Madison, WI, 39, 1990.
103. Russo, D. and Bresler, E., Scaling soil hydraulic properties of a heterogeneous field, *Soil Sci. Soc. Am. J.*, 44, 681, 1980.
104. Liu, H.H. and Molz, F.J. Multifractal analyses of hydraulic conductivity distributions, *Water Resour. Res.*, 33(11), 2483, 1997.
105. Sposito, G. and Jury, W.A., Miller similitude and generalized scaling analysis, in *Scaling in Soil Physics*, Hillel, D. and Elrick, D.E., Eds., Soil Science Society of America, Madison, WI, 13, 1990.
106. Miller, E.E. and Miller, R.D., Physical theory for capillary flow phenomena, *J. Appl. Phys.*, 27, 324–332.
107. Warrick, A. and Nielsen, D., Spatial variability of soil physical properties in the field, in *Applications of Soil Physics*, New York, Academic Press, Hillel, D., Ed., 1980.
108. Warrick, A. and Amoozegar, F., Infiltration and drainage calculations using spatially scaled hydraulic properties, *Water Resour. Res.*, 15, 1116, 1979.
109. Hillel, D., *Fundamentals of Soil Physics*, New York, Academic Press, 1980.
110. Tyler, S.W. and Wheatcraft, S.W., The consequences of fractal scaling in heterogeneous soils and porous media, in *Scaling in Soil Physics: Principles and Applications*, Hillel, D. and Elrick, E., Eds., Soil Sci. Soc. Amer. Special Pub.25. Madison, WI, 109, 1990.
111. Perrier E., Rieu, M., Sposito, G., and de Marsily, G., Models of the water retention curve for soils with a fractal pore size distribution. *Water Resour. Res.*, 32, 3025, 1996.

112. Dagan, G. and Bresler, E., Solute dispersion in unsaturated heterogeneous soil at field scale, I. Theory, *Soil Sci. Soc. Am. J.*, 413, 461, 1979.
113. Jury, W.A., Russo, D., and Sposito, G., The spatial variability of water and solute transport properties in unsaturated soil. II. Scaling models of water transport, *Hilgardia*, 55, 33, 1987.
114. Warrick, A.W., Mullen, G.J., and Nielsen, D.R., Scaling field measured soil hydraulic properties using a similar media concept, *Water Resour. Res.*, 13(2), 355, 1977.
115. Tidwell, V.C. and Wilson, J.L., Laboratory method for investigating permeability upscaling, *Water Resour. Res.*, 33(7), 1607, 1997.
116. Pyrak-Nolte, L.J., Nolte, D.D., and Cook, N.G.W., Hierarchical cascades and the single fracture: Percolation and seismic detection, in: *Fractals in Petroleum Geology and Earth Processes*, Barton, C.C. and La Pointe, P.R., Eds., Plenum Press, New York, 143, 1995.
117. Heffer and Koutsabeloulis, Fracture scale effects in hydrocarbon reservoirs, in: *Scale Effects in Rock Masses* 93, *Proc. 2nd Int. Workshop Scale Effects Rock Masses/Lisbon/Portugal/25 June, 1993*, 323, 1993.
118. Haken, H., *Advanced Synergetics: Instability Hierarchies of Self-Organizing Systems and Devices*, Berlin, New York: Springer-Verlag, 1983.
119. Slattery, J.C., *Momentum, Energy, and Mass Transfer in Continua*, New York, McGraw-Hill, 1972.
120. Yeh, T.-C.J., Scale issues of heterogeneity in vadose-zone hydrology, in *Scale Dependence and Scale Invariance in Hydrology*, Sposito, G., Ed., Cambridge University Press, New York, 1998.
121. Bear, J., *Dynamics of Fluids in Porous Media*, Elsevier, 1972.
122. Baveye, P. and Sposito, G., The operational significance of the continuum hypothesis in the theory of water movement through soils and aquifers, *Water Resour. Res.*, 20, 51, 521, 1984.
123. Pruess, K., Effective parameters, effective processes: from porous flow physics to *in situ* remediation technology, in: *Groundwater and Subsurface Remediation*, Kobus, H., Barczewski, B., and Koschitzky, H.P., Eds., Springer, Berlin, Heidelberg, New York, 183, 1996.
124. Tritton, D.J., *Physical Fluid Dynamics*, Oxford: Clarendon Press, 1988.
125. Sahimi, M., Flow, dispersion, and displacement processes in porous media and fractured rocks: from continuum models to fractals, percolation, cellular automata and simulated annealing, *Rev. Modern Phys.*, 65(4), 1393, 1993.
126. Baveye, P. and Sposito, G., Macroscopic balance equations in soils and aquifers: the case of space- and time-dependent instrumental response, *Water Resour. Res.*, 21, 1116, 1985.
127. Baveye, P. and Boast, C.W., Physical scales and spatial predictability of transport processes in the environment, in *Assessment of Non-Point Source Pollution in the Vadose Zone*, Corwin, D.L., Loague, K., and Ellsworth, T.R., Eds., Geophysical Monograph 108, American Geophysical Union, Washington, D.C., 261, 1998.
128. Neuman, S.P., Stochastic continuum representation of fractured rock permeability as an alternative to the REV and fracture network concepts, in: *Groundwater Flow and Quality Modeling*, E. Custodio, A. Gurgui, J.P. Lobo Ferreira, Eds., D. Reidel Publishing Company, 331, 1988.
129. Wood, E.F., Scale analyses for land surface hydrology, in *Scale Dependence and Scale Invariance in Hydrology*, Sposito, G., Ed., Cambridge University Press, Cambridge, 1, 1998.
130. Knutson, C.F., Cox, D.O., Dooley, K.J., and Sisson, J.B., Characterization of low-permeability media using outcrop measurements, in 68th Annual Technical Conference and Exhibition of the Society of Petroleum Engineers, October 3–6, 1993, Houston, TX, *SPE Paper 26487*, 1993.
131. Welhan, J.A. and Reed, M.F., Geostatistical analysis of regional hydraulic conductivity variations in the Snake River Plain aquifer, eastern Idaho, *GSA Bull.*, 109(7), 855, 1997.
132. Engelder, T., Joints and shear fractures in rock, in *Fracture Mechanics of Rock*, Atkinson, B.K., Ed., Academic Press, Orlando, FL, 27, 1987.
133. Priest, S.D., *Discontinuity Analysis for Rock Engineering*, Chapman and Hall, London, 1993.
134. Long, P. and Wood, B., Structures, textures, and cooling histories of Columbia River basalt flows, *Geol. Soc. Am. Bull.*, 97, 1144, 1986.
135. Nicolis, C., Predictability of the atmosphere and climate: towards a dynamical view, in *Space and Time Scale Variability and Interdependencies in Hydrological Processes*, Feddes, R.A., Ed., Cambridge [England]; New York, N.Y.: Cambridge University Press, 1995.
136. Likens, G.E., A priority for ecological research, *Bull. Ecol. Soc. Am.*, 64, 234, 1983.

137. Newman, M.E. and Dunnivant, F.M., Results from the large-scale aquifer pumping and infiltration test: transport of tracers through fractured media, *Idaho National Engineering Laboratory Report INEL-95/146 ER-WAG7-77*, 1995.
138. Wood, T.R. and Norrell, G.T., Integrated large-scale aquifer pumping and infiltration tests: groundwater pathways OU 7-06: summary report, *Idaho National Engineering Laboratory Report INEL-96/0256*, 1996.
139. Doughty, C., Numerical model of water flow in a fractured basalt vadose zone, Box Canyon site, Idaho, *Water Resour. Res.*, 36(12), 3521, 2000.
140. Dyer, J.R. and Voegele, M.D., High-level radioactive waste management in the United States background and status, in *Geological Problems in Radioactive Waste Isolation — Second World Wide Review*, Witherspoon, P.A., Ed., Lawrence Berkeley National Laboratory Report LBNL-38915, Lawrence Berkeley National Laboratory, Berkeley, CA, 259, 1996.
141. Rousseau, J.P., Kwicklis, E.M., and Gillies, D.C., Eds., Hydrogeology of the unsaturated zone, north ramp area of the exploratory studies facility, Yucca Mountain, Nevada. *Water Resour. Invest. Rep. 98-4050*. Denver, Colorado: U.S. Geological Survey, 1998.
142. Bodvarsson, G.S., Boyle, W., Patterson, R., and Williams, D., Overview of scientific investigations at Yucca Mountain — the potential repository for high-level nuclear waste, *J. Contam. Hydrol.*, 38, 3, 1999.
143. Mongano, G.S., Singleton, W.L., Moyer, T.C., Beason, S.C., Eatman, G.L.W., Albin, A.L., and Lung, R.C., Geology of the ECRB cross drift – exploratory studies facility, yucca mountain project, Yucca Mountain, Nevada, Bureau of Reclamation and U.S. Geological Survey, Denver, Colorado, 1999.
144. Bandurraga, T.M. and Bodvarsson, G.S., Calibrating hydrogeologic parameters for the three-dimensional site-scale unsaturated zone model of Yucca Mountain, Nevada, *J. Contaminant Hydrol.*, 38(1-3), 25, 1999.
145. Montazer, P. and Wilson, W.E., Conceptual hydrologic model of flow in the unsaturated zone, Yucca Mountain, Nevada, U.S. Geological Survey, *Water Resour. Invest. Rep.* 84-4345, Lakewood, CO, 1984.
146. Barton, C.C. and Larsen, E., Fractal geometry of two-dimensional fracture networks at Yucca Mountain, southwest Nevada, in *Fundamentals of Rock Joints: International Symposium on Fundamentals of Rock Joints*, Stephansson, O., Ed., Bjorkliden, Lapland, Sweden, Centek Publishers, Lulea, Sweden, Proceedings, 77, 1985.
147. Kumar, S. and Bodvarsson, G.S., Fractal study and simulation of fracture roughness. *Geophys. Res. Lett.*, 17, 701, 1990.
148. Nolte, D.D., Pyrak-Nolte, L.J., and Cook, N.W.G., The fractal geometry of flow paths in natural fractures in rock and the approach to percolation, *Pure Appl. Geophys.*, 131(1/2), 111, 1989.
149. Cox, B.L. and Wang, J.S.Y., Fractal analysis of anisotropic fracture surfaces, *Fractals*, 1(13), 547, 1993.
150. La Pointe, P.R., A method to characterize fracture density and connectivity through fractal geometry, *Int. J. Rock Mech. Min. Sci. Geotech. Abs.*, 25(6), 421, 1988.
151. Nieder-Westermann, G.H., Fracture geometry analysis for the stratigraphic units of the repository host horizon, ANL-EBS-GE-000006 Rev 00. CRWMS M&O: Las Vegas, Nevada, 2000.
152. Wu Y.-S., Haukwa, C., and Bodvarsson, G.S., A site-scale model for fluid and heat flow in the unsaturated zone of Yucca Mountain, Nevada, *J. Contaminant Hydrol.*, 38(1-3), 185, 1999.
153. Ahlers, C.F., Finsterle, S., and Bodvarsson, G.S., Characterization and prediction of subsurface pneumatic response at Yucca Mountain, Nevada, *J. Contaminant Hydrol.*, 38(1-3), 47, 1999.
154. Cook, P., *In situ* pneumatic testing at Yucca Mountain, *Int. J. Rock Mech. Min. Sci.*, 37, 357, 2000.
155. Bodvarsson, G.S., Ahlers, C.F., et al., Unsaturated zone flow and transport model process model report, LBNL, 2000.
156. Salve, R. and Oldenburg C.M., Water flow in a fault in altered nonwelded tuff, *Water Resour. Res.*, 37, 3043, 2001.
157. Salve, R., Wang, J.S.Y., and Doughty, C., Liquid release tests in unsaturated fractured welded tuffs: I. field investigations, *J. Hydrol.*, 256, 60, 2002.
158. Wang, J.S., Cook, P.J., Trautz, R.C., et al., *In situ* field testing of processes, ANL-NBS-HS-000005, Rev. 01, 2001.
159. Kneafsy, T.J. and Pruess, K., Laboratory experiments on heat-driven two-phase flows in natural and artificial rock fractures, *Water Resour. Res.*, 34(12), 3349, 1998.

160. Doughty, C., Salve, R., and Wang, J.S.Y., Liquid release tests in unsaturated fractured welded tuffs: II. Numerical modeling. *J. Hydrol.*, 256, 80, 2002.
161. Eliassi, M. and Glass, R.J., On the continuum-scale modeling of gravity-driven fingers in unsaturated porous media: the inadequacy of the Richards equation with standard monotonic constitutive relations and hysteretic equations of state, *Water Resour. Res.*, 37(8), 2019, 2001.
162. Liu, H.H., Doughty, C., and Bodvarsson, G.S., An active fracture model for unsaturated flow and transport in fractured rocks, *Water Resour. Res.*, 34(10), 2633, 1998.
163. Barenblatt, G.I., *Scaling, Self-similarity, and Intermediate Asymptotics*, New York: Cambridge University Press, 1996.
164. Robinson, B.A. and Bussod, G.Y., Radionuclide transport in the unsaturated zone at Yucca Mountain: numerical model and field validation studies, in *Geophysical Monograph No. 122: Dynamics of Fluids in Fractured Rock*, Faybishenko, B., Witherspoon, P.A., and Benson, S.M., Eds., 323, 2000.
165. LeCain, G.D., Results from air-injection and tracer testing in the upper Tiva Canyon, Bow Ridge Fault, and upper Paintbrush contact alcoves of the exploratory facility, August 1994 through July 1996, Yucca Mountain, Nevada. *Water Resour. Invest., Rep.* 98–4058. Denver, Colorado: U.S. Geological Survey, 1998.
166. Hsieh, P.A., Scale effects in fluid flow through fractured geologic media, in *Scale Dependence and Scale Invariance in Hydrology*, Sposito, G., Ed., Cambridge University Press, New York, 335, 1998.
167. Pruess, K., A mechanistic model for water seepage through thick unsaturated zones in fractured rocks of low matrix permeability, *Water Resour. Res.*, 35(4), 1039, 1999.
168. Gauthier, J.H., Wilson, M.L., and Lauffer, F.C., Estimating the consequences of significant fracture flow at Yucca Mountain, in *Proc. 3rd Annu. Int. High-Level Radioactive Waste Manage. Conf.*, Las Vegas, NV, American Nuclear Society, La Grange Park, IL, vol. 1, 891, 1992.
169. Jury, W.A. and Roth, K., *Transfer Functions and Solute Movement through Soil: Theory and Applications*, Birkhäuser Verlag, Basel, Switzerland, 1990.
170. Babchin, A.J., Frenkel, A.L., Levich, B.G., and Sivashinsky, G.I., Flow-induced nonlinear effect in thin film stability, *Ann. NY Acad. Sci.*, 404, 426, 1983.
171. Frenkel, A.L., Babchin, A.J., Levich, B., Shlang, T., and Sivashinsky, G.I., Annular flows can keep unstable films from breakup: nonlinear saturation of capillary instability, *J. Colloid Interface Sci.*, 115, 225, 1987.
172. Schuster, H.G., *Deterministic Chaos: an Introduction*, Weinheim, Federal Republic of Germany : Physik-Verlag; New York, 1989.
173. Sposito, G., On chaotic flows of water in the vadose zone, *Abstracts of the Fall 1999 AGU Meeting*, December 1999.
174. Nicholl, M.J. and Detwiler, R.L., Simulation of flow and transport in a single fracture: macroscopic effects of underestimating local head loss. *Geoph. Res. Lett.*, 28(23), 4355, 2001.
175. Nikolaevskij, V.N., *Mechanics of Porous and Fractured Media*, World Scientific, Singapore, 1990.
176. Landau, L.D. and Lifshitz, E.M., *Fluid Mechanics*, 2nd ed., Series *Course of Theoretical Physics*, Vol. 6, Pergamon Press, Oxford, England; New York, 1987.
177. Hallaire, M., Irrigation et utilisation reserves naturelles, *Ann. Agric.*, 12, 1, 1961.
178. Rode, A.A., *Osnovy Ucheniia o Pochvennoi Vlage (Theory of Soil Moisture)*, Leningrad, Gidrometeorologicheskoe izd-vo, v.1., 1965.
179. Feldman, G.M., *Water Movement in Thawing and Freezing Soils*, Novosibirsk, Nauka, Sibirskoe otdnie, 1988.
180. Doughty, C., Investigation of conceptual and numerical approaches for evaluating moisture, gas, chemical, and heat transport in fractured unsaturated rock, *J. Contaminant Hydrol.*, Special Issue, 38, 69, 1999.
181. Bodvarsson, G.S., Bandurraga, T.M. and Wu, Y.S., The site-scale unsaturated zone model of Yucca Mountain, Nevada, for the viability assessment, Technical Report LBNL-40378, Lawrence Berkeley National Laboratory, 1997.
182. Robinson, B.A. et al., The site-scale unsaturated zone transport model of Yucca Mountain, Yucca Mountain Site Characterization Project, Milestone Report SP25BMD, Los Alamos, New Mexico, Los Alamos National Laboratory, 1997.
183. Nitao, J.J. and Buscheck, T.A., Infiltration of liquid front in an unsaturated, fractured porous medium, *Water Resour. Res.*, 27(8), 2099, 1991.

184. Wang, J.S.Y. and Narasimhan, T.N., Hydrologic mechanisms governing fluid flow in a partially saturated, fractured, porous medium, *Water Resour. Res.*, 21(12), 1861, 1985.
185. Wang, J.S.Y. and Narasimhan, T.N., Unsaturated flow in fractured porous media, in *Flow and Contaminant Transport in Fractured Rock*, J. Bear, C.-F. Tsang, G. DeMarsily, Eds., Academic Press, NY, 1993.
186. Eaton, R.R., Ho, C.K., Glass, R.J., Nicholl, M.J., and Arnold, B.W., Three-dimensional modeling of flow through fractured tuff at Fran Ridge, Sandia National Laboratories, Albuquerque, NM, 1996.
187. Wittwer, C., Chen, G., Bodvarsson, G.S., Chornack, M., Flint, A., Flint, L., Kwicklis, E., and Spengler, R., Preliminary development of the LBL/USGS three-dimensional site-scale model of Yucca Mountain, Nevada, Report LBL-37356/UC-814, 1995.
188. Birdsell, K.H., Wolfsberg, A.V., Hollis, D., Cherry, T.A., and Bower, K.M., Groundwater flow and radionuclide transport calculations for a performance assessment of a low-level waste site, *J. Contam. Hydrol.*, 46(1-2), 99, 2000.
189. Buscheck, T.A. and Nitao, J. J., Repository-heat-driven hydrothermal flow at Yucca Mountain. I. Modeling and analysis, *Nucl. Technol.*, 104, No. 3, 418, 1993.
190. Sonnenthal, E.L. and Bodvarsson, G.S., Constraints on the hydrology of the unsaturated zone at Yucca Mountain, NV, from three-dimensional models of chloride and strontium geochemistry, *J. Contaminant Hydrol.*, 38 (1-3), 107, 1999.
191. Fabryka-Martin, J.T., Flint, A.L., Sweetkind, D.S., Wolfsberg, A.V., Levy, S.S., Roach, J.L., Woldegabriel, G., and Wolfsberg, L.E., Evaluation of flow and transport models of Yucca Mountain, based on chlorine-36 studies for FY97. Los Alamos Report LA-CST-TIP-97-010, LANL Milestone SP2224M3. Los Alamos, NM, Los Alamos National Laboratory, 1997.
192. Rodriguez-Iturbe, I., Entekhabi, D., and Bras, R.L., Nonlinear dynamics of soil moisture at climate scales: 1. Stochastic analysis, *Water Resour. Res.*, 27(8), 1899, 1991.
193. Rodriguez-Iturbe, I., Entekhabi, D., Lee, J.S., and Bras, R.L., Nonlinear dynamics of soil moisture at climate scales: 2. Chaotic analysis, *Water Resour. Res.*, 27(8), 1907, 1991.
194. Hinds, J.J. and Bodvarsson, G.S., Role of fractures in processes affecting potential repository performance. LBNL-47039 (presentation given at the 2001 International High-Level Radioactive Waste Management Conference, Las Vegas.)